Electron Bombardment Induced Conductivity

and its applications

IPR2014-00580
Gillette v. Zond
GILLETTE 1026

Electron Bombardment Induced Conductivity
and its applications

by

The late W. EHRENBERG
Formerly Emeritus Professor of Physics
Birkbeck College
University of London, U.K.

and

D. J. GIBBONS
Central Research Laboratories
THORN EMI plc
Hayes, Middlesex, U.K.

1981

ACADEMIC PRESS
A Subsidiary of Harcourt Brace Jovanovich, Publishers
London New York Toronto Sydney San Francisco

QC610 .4 .E37 1981

ACADEMIC PRESS INC. (LONDON) LTD
24/28 Oval Road,
London NW1

United States Edition published by
ACADEMIC PRESS INC.
111 Fifth Avenue,
New York, New York 10003

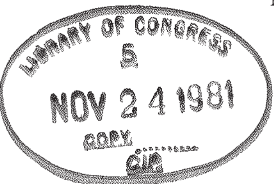

Copyright © 1981 by
ACADEMIC PRESS INC. (LONDON) LTD

All rights reserved
No part of this book may be reproduced in any form by photostat, microfilm, or any other means, without written permission from the publishers

British Library Cataloguing in Publication Data

Ehrenberg, W.
Electron bombardment induced conductivity and its applications.
1. Electric conductivity 2. Electron beams
I. Gibbons, D. J.
537.6′2 0C610.4

ISBN 0–12–233350–0
LCCCN 81–66385

Printed by W & G Baird Ltd at The Greystone Press, Antrim

Preface

This is the first book to be written in which the subject matter is dedicated exclusively to electron bombardment induced conductivity. The treatment presented is suitable for the graduate or final-year undergraduate physicist, materials scientist or electronic engineer whose interests lie in the electronic properties of insulators or semiconductors or in the design and development of electron devices. Recent developments such as time-of-flight techniques and the scanning electron microscope are dealt with and, as this is the first publication of its kind, we have not only reviewed these but we have found it necessary to examine critically the foundations upon which the more recent studies and applications are now standing. However, the reader might then have been left with an almost intolerable burden of work if we had merely provided a long list of references, so we have attempted to incorporate the information supplied by the relevant authors as part of the overall story.

In the early years, the influence on the electrical conductivity of an insulator or semiconductor while bombarded by fast electrons (electron bombardment conductivity, or EBC) was treated in its own right in a very similar way to the closely related phenomena of photoconductivity and cathodoluminescence. The studies were largely phenomenological, and the greater part of the first few chapters treats EBC from this standpoint. However, the subject has now progressed to the stage where a somewhat more theoretical approach is necessary for interpreting the observations correctly. Such is the case where transient EBC methods are used for characterizing an insulating or semiconducting material. Some workers call these drift mobility techniques, and two chapters are devoted to this important application of EBC. But derivation of most of the mathematical formulae has been omitted here.

The equivalent phenomenon to the photovoltaic effect is known as the electron voltaic effect (EVE). Large non-permanent changes in the conductivity of semiconductor barriers have been applied in electron devices, where an electron bombarded p–n junction or Schottky barrier structure in a semiconductor target has been used to achieve virtually noise-free current amplification. Such electron bombarded semiconductor targets were first used extensively in the 1970s, and further work can be expected soon when radiation hardened semiconductor devices become more common.

An important new application has arisen recently because of the scanning electron microscope. In the electron beam induced current mode, an image of sub-surface structures (such as bulk defects, or dislocations) can be examined by collecting the charge carriers released internally by the beam. The corresponding current is used as a video signal. A brief description of this application is made in the ultimate chapter.

The book was completely planned and most of the earlier parts had been written when the senior author died. His untimely death has left the scientific community the poorer for the loss of a brilliant scientist. His interest in the subject extended for almost 40 years and it continued right up to a few days before he passed away. Among his particular attributes was an insistence on understanding the underlying physical reason for certain patterns of EBC behaviour, and his ability to overcome irritating practical difficulties which always confront the experimentalist. The book includes a number of such seemingly small details which have been found important from experience. The basic philosophy behind the approach adopted in the book, and which was agreed by the authors at the outset, has been maintained throughout.

Grateful thanks are expressed to Professor W. E. Spear who read most of the manuscript and to whom the authors are indebted for many corrections and suggestions. Thanks are also due to Dr J. Hirsch and Dr E. W. Williams who assisted in reading some portions of the manuscript. Finally, the untiring assistance of Mrs M. Johnson of the THORN EMI central library, and of my wife Jean, with the references has been much appreciated.

June 1981 D. J. Gibbons

Contents

Preface

Chapter 1. Physical principles of electron bombardment conductivity (EBC)

I. Historical background, 1
II. Energy levels in solids, 5
  A. Crystalline solids, 5
  B. Amorphous solids, 9
  C. Localized energy states, 11
III. Conduction of electricity through insulators, 17
  A. Conduction of electricity through gases, 17
  B. Transport of electrons and holes through crystals, 20
  C. Transport of electrons and holes through amorphous solids and low mobility crystals, 24
  D. Drift experiments in gases or in insulating solids and liquids, 32

Chapter 2. Properties of electron beams and their interaction with matter

I. Sources of electrons, 34
  A. Radioactive sources, 34
  B. Electron guns for EBC measurements, 34
  C. EHT supplies, 41
  D. Concentration of intensity with electron lenses, 41
  E. Transmission of control, 42
  F. The scanning electron microscope (SEM), 43
II. Path length and energy loss of fast electrons, 43
  A. Cloud chamber tracks, 44
  B. Thomson–Whiddington–Bethe law of energy losses, 44
  C. The problem of penetration, 49
  D. Experimental measurements using phosphorescence glows, 54
  E. Scaling of variously defined ranges, 59
  F. Range–energy tables, 60
  G. Range measurements on primary electrons of energy below about 10 keV, 61
III. Ionizing radiation and radiation effects, 65
  A. Production of electron–hole pairs, 65
  B. Luminescence, 67

C. Photoconduction, 67
D. Photovoltaic effect, 70
E. Radiation damage, 71
F. Cosmic rays, 75
G. Nuclear radiation, 77
H. Persistent polarization, 78

Chapter 3. Steady state EBC of thin insulating films
I. Preparation of films, 80
A. Evaporation, 80
B. Sputtering, 81
C. Glassy bubbles, 81
D. Deposition by glow discharge, 82
E. Anodizing and chemical deposition, 83
F. Other methods, 84
II. Specimens for measurements, 84
A. Solid electrodes, 86
B. Electron beam contacts, 86
III. Transfer of excitation, 89
A. X-rays, 89
B. Excitons, 90
C. Fluorescence, 91
IV. Conductivity induced by electrons, 92
A. Influence of bombarding voltage, 93
B. Gain, 103
C. Lateral induced conductivity, 114
D. The influence of contacts in normal EBC, 121

Chapter 4. The electron voltaic effect (EVE)
I. Semiconductor junctions, 123
A. Point contacts, 125
B. Schottky barriers, 125
C. p–n junctions, 128
II. Practical junctions, 129
A. Theory of the EVE, 129
B. Diffusion length of conduction electrons in silicon solar cells, 132
III. Particular semiconductor junctions, 133
A. Selenium, 133
B. Gallium arsenide, 135
C. Silicon, 135
D. EBC avalanche effect, 137

Chapter 5. Transient EBC time-of-flight measurements
I. Time-of-flight technique, 141
A. Background of similar work prior to 1957, 142
B. Measurements on a crystal in its virgin state, 143
C. Types of transient EBC measurements, 144
D. Comparison with light-flash or α-particle excitation, 158
E. Insulators having a short carrier free lifetime, 160
F. Semiconductors having a short dielectric relaxation time, 161
G. Signal averaging, 164
II. Transient EBC methods for measurements other than drift velocity, 165
A. Transient EBC pulse shape near $t = 0$, 165
B. Electric field profiles, 166
C. Carrier recombination, 166
D. Mean free carrier lifetime, 168
E. Amorphous semiconductors and the continuous time random walk, 170
F. Trap distributions, 173
G. Carrier release time from traps, 175
III. Carrier velocity, 177
A. Mobility of either sign of carrier, 177
B. Trap-controlled mobility, 180
C. Trap density, 181
D. The motile trap model, 182
IV. Apparatus, 183
A. Medium and low mobility insulating solids and liquids, 183
B. Solid gases, 186
C. High mobility solids, 188
D. Microwave time-of-flight technique, 192

Chapter 6. Specific materials properties determined by transient EBC techniques
I. Group IV elemental semiconductors, 196
A. Silicon, 196
B. Germanium, 201
C. Diamond, 206
II. Amorphous silicon, 208
III. III–V intermetallic compound semiconductors, 222
A. Gallium arsenide, 223
B. Indium antimonide, 226
IV. II–VI compounds, 228
A. Cadmium sulphide, 228

B. Cadmium telluride, 235
C. Other II–VI solids, 241
V. Solid and liquid gases, 244
A. Noble gases (neon, argon, krypton, and xenon), 244
B. Molecular gases (nitrogen, oxygen, carbon monoxide, hydrogen, and methane), 250
VI. Selenium and sulphur, 254
A. Selenium, 254
B. Sulphur, 256

Chapter 7. Applications of EBC and EVE in electron devices
I. Devices using semiconductor junctions, 265
A. Photosil EVE hybrid multiplier photocell, 265
B. Digicon multichannel photocell, 269
C. Intensified charge coupled devices (ICCD) and self-scanned arrays, 274
D. Silicon intensifier target (SIT) television pickup tube and SIT scan converter, 279
E. Evoscope fixed pattern generator, 284
F. Electron bombarded semiconductor (EBS) microwave devices, 285
G. Degradation phenomena, 291
II. Miscellaneous applications of bombarded semiconductor targets, 294
A. Barrier EVE and the scanning electron microscope, 294
B. Nuclear radiation detectors, 305
III. EBC of insulating films in electron devices, 311
A. Ebicon (Ebitron, Uvicon) television pickup tube, 311
B. Computer mass memory (Beamos, Ebam), 313
C. Graphechon scan converter, 317

Appendix
I. Two-layer dielectric, 321
II. Secondary emission of insulators, 322
III. Optimum scanning speed for constant charge imaging device, 323
IV. Ramo's theorem, 325

References, 327

Index, 340

1

Physical principles of electron bombardment conductivity (EBC)

I. Historical background

The study of EBC is concerned with the conduction of electricity across gaps between electrodes. The gaps may be filled by a non-metallic solid and only a very small current can flow in the presence of an applied electric field if the electrodes are blocking. However, conductance can often be influenced by radiation, particularly electromagnetic rays, cathode rays, and nuclear particles. The effect of the first—photoconductivity—was discovered about 100 years ago and for many years it was considered to be the property of only a few substances. In Glazebrook's classic *Dictionary of Applied Physics* (1922) for example we read: "Arrhenius (1887) showed that by exposing silver halides to light an increase in electric conductivity was produced . . . various other substances have been studied by Coblentz and Emerson. The well-known sensitiveness of selenium to light, shown by a diminution in electrical resistance when thin films are illuminated, may be explained by supposing that the *incident light liberates slowly moving electrons* which remain within the substance and increase its conducting power". Actually the generation of an emf in a galvanic cell when one of its plates was illuminated by violet light was discovered by E. Becquerel (1839) in the form we now know as the photovoltaic effect. The photoconductive effect was discovered by Willoughby Smith (1873) who accidentally came across it in selenium. In 1916 it was discovered in cuprous oxide, and from then onwards a systematic search led to the discovery of many more photoconductive materials, in particular sulphides and coloured alkali halides.

Studies of the influence of X-rays and nuclear particles from sources such as uranium or radium were made towards the end of the 19th century. Within a year of Röntgen's (1895) discovery of X-rays, J. J. Thomson showed that the paraffin wax dielectric of a condenser became conducting under their influence. Curie showed that radium can cause insulating liquids to become conductive (1895), and H. Becquerel found that uranium can produce a similar effect in gases (for early history of these effects see

3

Steady state EBC of thin insulating films

By the term "thin films" we mean those that are sufficiently thin to allow the primary electrons to penetrate them completely at the highest accelerating voltage used for the experiment. Of crystals, only mica and selenite can be cleaved thin enough to qualify as films; neither shows a strong EBC response. Attempts to lap down crystals usually result in cracking them when they are less than 50 μm thick. Several authors have described attempts to wash down single crystals of alkali halides by dissolving selected regions by a small jet of saturated aqueous solution, but generally such methods still caused cracking.

I. Preparation of films

In recent years many advances have been made in developing new techniques for producing thin films of insulators, semiconductors, and metals. It is beyond the scope of this book to describe these in sufficient detail to be useful, and the reader is referred to the excellent book edited by Vossen and Kern (1978). The few methods about to be described were well established in about 1948 when studies of EBC were started, and they are included here to provide a background to the available techniques used by most experimentalists in the years between then and about 1970. One exception is the glow discharge decomposition of silane (SiH_4) which has become of importance for producing high resistivity amorphous thin films of silicon; this will be described below in Section D.

A. Evaporation

The most common process for producing thin films is by evaporation in a good vacuum. The evaporation "boat" can be made from a 40 mm length of tantalum or molybdenum sheeting about 0·1 mm thick × 10 mm wide; a heavy current transformer is used to pass the heating current through the

boat. The residual gas pressure in the evaporation chamber should be less than about 10^{-5} torr during evaporation, and much spitting and showering of the evaporant from the boat is avoided if it is preheated gradually while the vacuum pump is reducing the pressure. The boat should be provided with a "dimple" in its centre to accommodate the material being evaporated, which is usually in a pure finely powdered dry state, although single crystals or a compressed pellet can be used.

Suitable substrates for the films can be glass microscope slides carefully selected for the absence of small surface scratches. Even better substrates are made from ground and polished glass discs cleaned in a mixture of sulphuric acid and hydrogen peroxide, washed in distilled water, and dried in hot trichlorethane vapour. Occasionally the substrate should be heated in order to improve stoicheiometry in those cases where decomposition takes place during evaporation; examples of compounds to which this applies are CdS and ZnS. Masks to limit the extent of the layer can be made from stainless steel, and occasionally mechanical masking arrangements are used so that they can be changed without breaking the vacuum if electrodes are also evaporated.

B. Sputtering

Some layers can be deposited by sputtering in an inert atmosphere. The material is compressed into a thin disc about 0·5 mm thick and held on aluminium or steel by a pressure bond. The metal disc, hung horizontal by a hook on a vertical conducting wire which enters from the top of a glass bell-jar, is kept at a distance of about 10 cm from the substrate. The bell-jar is first evacuated; while still pumping, argon gas is allowed to enter the bell-jar through a needle valve and the equilibrium pressure is adjusted to lie between about 1 and 0·01 torr. This continuous flow method tends to sweep away any impurities that might be desorbed from the electrodes during deposition.

Sputtering takes place when a high voltage is applied between the substrate and cathode. A dc voltage of around 5–20 kV is sufficient, and this should be applied to the metal disc (which is negative) through a resistor of about 1 megohm; the substrate is at earth potential. The discharge glow can be limited to a particular volume by surrounding the space between anode and cathode by a glass cylinder.

C. Glassy bubbles

Glasses can be blown as thin bubbles. For example, molten As_2S_3 can be blown as a bubble on the end of a Pyrex tube, using a controlled flow of dry

nitrogen inside a glove-box filled with nitrogen. When cold, such bubbles can be used by cutting small regions which are not too far from being flat. Ordinary glass such as Pyrex is too conductive to show a response to electron bombardment but thin bubbles blown in air were used successfully by Spear and Mort (1963) to make blocking contacts to CdS under pulsed electron excitation.

D. Deposition by glow discharge

An rf or dc glow discharge in an atmosphere of silane (SiH_4) can be used to produce layers of amorphous silicon (a-Si) up to about 3 μm thick. The excitation may be either from an rf coil or between parallel planar electrodes; the latter method provides larger area films of greater uniformity. Suitable apparatus is shown in Fig. 3.1. The gas pressure is reduced by means of a vacuum pump fitted with a throttle valve so that the equilibrium pressure is about 0·1–1 torr. Stimulation is provided by a 500 W oscillator operating at 1 MHz; although the rated power is much higher, the actual discharge is run at a power of 10–20 W. Substrates placed in the glow so produced, which remains in close contact with the specimen surface, are coated at a rate of about 1 Å per second. The substrate is usually heated because the properties of the amorphous silicon depend critically on this temperature.

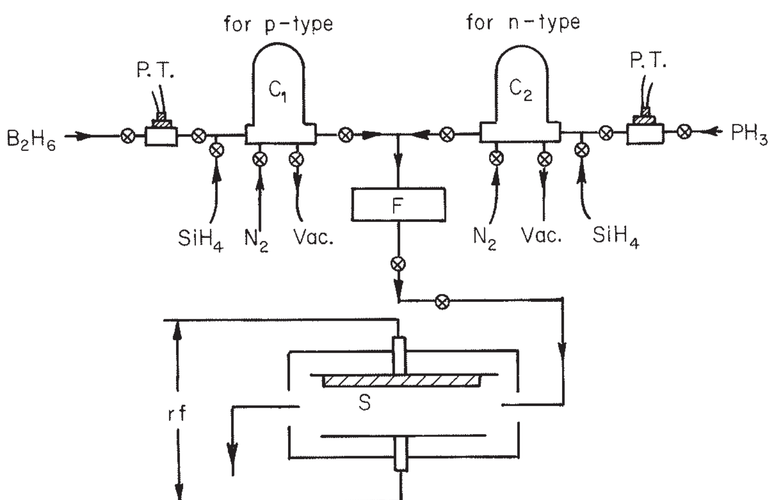

Figure 3.1. Schematic diagram of the preparation unit for n- and p-type a-Si. C_1 and C_2, glass cylinders; P.T., pressure transducers; F, flow meter; S, substrate. (Le Comber and Spear, 1979)

Glow discharge a-Si can be doped with phosphorus or with boron by adding controlled amounts of PH_3 or B_2H_6 to the starting gas. It is thus possible to produce substitutionally doped n-type or p-type a-Si. The equipment for this process is also shown in Fig. 3.1 (Le Comber and Spear, 1979). Glow discharge a-Si is in fact a hydrogen-compensated amorphous semiconductor, the hydrogen effectively saturating (or nearly saturating) the dangling bonds.

E. Anodizing and chemical deposition

Oxide films can be grown on some metals such as aluminium and tantalum. The anodized film on aluminium has received some attention because it shows appreciable induced conductivity; such films have a complicated structure. Tantalum oxide films are also fairly good EBC insulators.

The method employed to form good EBC films of Al_2O_3 was described by Ansbacher (1950) as follows. The pure aluminium foil about 40 μm thick was cleaned by immersing it for about 5 min in a nearly boiling solution of 20 g of CrO_3 in 35 ml of H_3PO_4 (specific gravity 1·72) made up to 1 litre with distilled water. After rinsing in distilled water, the samples were anodized by the chromic acid process in a 3% Cr_2O_3 solution at 40°C. The cathode was a carbon rod and all the wires and other fixtures were of aluminium. The current density was 5 mA cm^{-2} at the start but it rapidly died down. During the first 15 min the voltage was raised from zero to 45 V and then kept at 45 V for a further 40 min; finally it was raised to 50 V or more for 5 min. Samples produced with up to 135 V final anodizing voltage were used. The thickness of the oxide layer could be determined from optical interference fringes at the edges.

After anodizing, the metal-based specimen was washed, dried, and fitted with a thin vacuum-evaporated aluminium electrode over its surface. Alumina films produced by the chromic acid anodizing process have a higher EBC gain than those produced by the tartaric acid process or Al_2O_3 films produced by sputtering.

Films of tantalum oxide may be grown by anodizing pure tantalum sheet in 0·02 M phosphoric acid solution, the ultimate thickness being determined fairly precisely by the anodizing voltage; Aris *et al.* (1976) describe the EBC of such films in the thickness range 72–360 nm.

If thermal decomposition is severe, vacuum evaporation cannot be used. Chemical methods can be employed to prepare thin films in some instances. Pensak (1948) prepared thin films of SiO_2 by heating Nichrome base plates to about 700°C in the presence of ethyl silicate vapour. It is interesting that even today the highest purity synthetic silica is still produced by hydrolysis of ethyl silicate vapour in a similar way.

Thin films of ZnO can be prepared by evaporating zinc in a good vacuum and subsequently oxidizing by baking in air or oxygen for 5 min at 400°C, and thin (polycrystalline) layers of PbO can be produced by evaporating PbO from a platinum crucible through oxygen at a pressure of 10^{-2} torr on to a substrate held at 110°C.

F. Other methods

Under this heading we include techniques that were little known, or even unknown, when studies of EBC were started seriously. Even though some of these techniques evolved while such studies were in progress, the older methods were often still employed, so a direct comparison of different properties of similar films produced by the same techniques could be made in the same laboratory. The available technologies for producing thin films now include chemical etching, plasma deposition of inorganic films, glow discharge polymerization, ion beam deposition, magnetron sputtering, sputter gun deposition, glow discharge sputter deposition, and electron beam evaporation. For details of these, the reader is referred to the book edited by Vossen and Kern (1978).

II. Specimens for measurements

Specimens of an insulator for EBC measurements are usually prepared in the form of a metal–insulator–metal sandwich. The contact on the side of the thin film remote from the electron source is usually a conducting film of metal deposited on a glass substrate, although in some instances it can be the substrate itself (e.g. Ta or Al), or self-supporting (or weakly supported) films can be prepared for electron beam access from either side.

A typical arrangement is shown in Fig. 3.2. In this example, a gold or aluminium back electrode is vacuum evaporated on to a cleaned glass microscope slide using a brass or stainless steel mask to limit the size of the conductive area. Good electrical contact can be made to this at a later stage if a strip of Aquadag is painted on one edge of the glass beforehand and, after drying the Aquadag in a warm place, the metal layer is evaporated on to this layer also. Such contacts are more reliable than those made with Aquadag after metallizing.

The specimen (insulator or semiconductor) is deposited over an area slightly larger than that of the bottom electrode, again using an appropriate mask. If the edges of this film are slightly diffuse it is often possible to measure the thickness by the Tolansky interferometric method.

The top electrode is now evaporated on to the insulator, but this time the contact point is brought out on the opposite edge of the glass slide so that

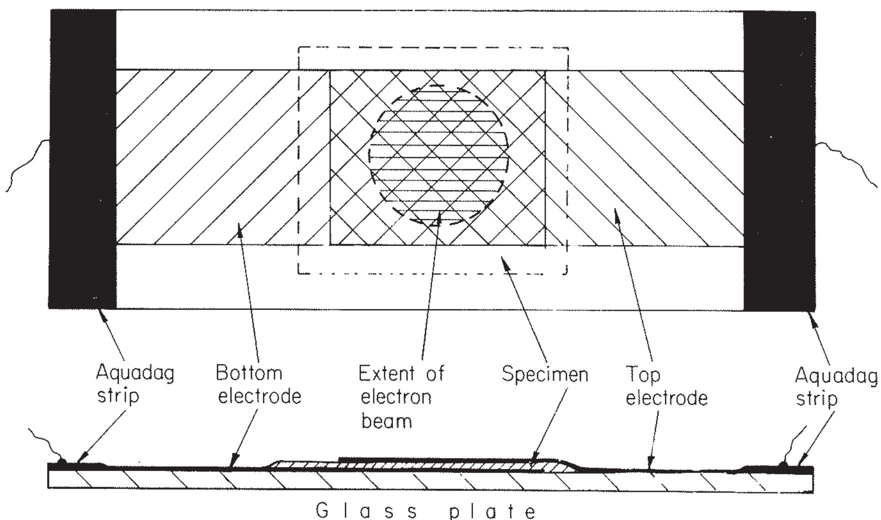

Figure 3.2. Diagram showing a mounted specimen prepared for measurements of steady-state EBC; the contact wires at each side are of 0·1 mm diameter copper and are joined to the Aquadag with silver paste.

short-circuits between the top and bottom metal electrodes are avoided. Of course, if the top contact is an electron beam the surface of the insulator is left free.

If the insulator is to be weakly supported it can be vacuum evaporated on to a thin alumina membrane made by the tartaric acid anodizing process (Harris, 1955).

Films completely open on both sides can be made by vacuum evaporation on to copper foil; the copper can then be removed, if the insulator is not attacked, by carefully dropping a spot of concentrated nitric acid on to the foil (Spear, 1955). An alternative method if the insulator is not damaged by heat is to evaporate it on to a thin "skin" of nitrocellulose supported on a fine-pitch electroformed metal grid (e.g. 20 threads per mm). Such substrates can be made by dropping a spot of nitrocellulose in ethyl acetate (Collodion) on to the surface of water in a vertical-sided trough. When the solvent evaporates, the floating nitrocellulose membrane can be picked up on the metal grid, which is mounted on a frame immersed in the water, by slowly raising it at an angle of 45° through the surface. After drying it and evaporating the insulator, the nitrocellulose can be destroyed by baking the specimen in air or in a vacuum at 400°C for 30 minutes. Other workers have reported a technique whereby the insulator is evaporated on to a smooth rock-salt surface which is subsequently removed by dissolving it in water.

A. Solid electrodes

If the primary electrons penetrate the front (top) electrode of a thin metal–insulator–metal sandwich film, this contact should be electrically continuous and have very little stopping power at the bombarding voltage (V_p) used. For this reason aluminium is often chosen; the thickness should be about 1000 Å. This metal can be readily evaporated in a vacuum better than 10^{-5}–10^{-6} torr from a helix about 8 mm in diameter made from 1 mm tungsten wire or, better still, from a multiple strand of three tungsten wires 0·5 mm thick twisted together. Pure and clean aluminium wire 1 mm in diameter is cut into pieces about 10 mm long and bent into horseshoe shapes, and these are crimped around the tungsten wire at 5–10 mm intervals with pliers. The aluminium evaporates from the tungsten in a high vacuum when it is electrically heated to about 1000°C by passing a current through it. The substrate is typically at a distance of 15–25 cm from the source.

Alternatively an evaporated gold contact is used; this should be 350–400 Å thick. A suitable source is a 5 mm diameter helix, 5 cm long, of stranded wire made by twisting together three lengths of 0·5 mm tungsten and one of gold wire. The tungsten wire is cleaned before use by an electrolytic method using the wire as anode and a solution made up from 25 g of NaOH and 100 g of Na_3PO_4 in 2 litres of water as electrolyte at about 85°C.

If aluminium or gold are unsuitable, an Aquadag electrode can often be painted on. Wetting of the specimen is aided by adding a wetting agent such as Teepol to the aqueous dispersion or by selecting one of the dispersions that are available in an organic medium such as ethanol.

B. Electron beam contacts

Electron beam contacts can be explained by reference to a particular example. Suppose a target made of some insulating material is mounted at one end of a tube facing an electron gun; surrounding the target is a collector electrode by which secondary electrons emitted by the target may return to earth. Such a tube is shown diagrammatically in Fig. 3.3(a). Consider what happens when the cathode of the electron gun is at earth potential and the collector potential (V_{coll}) is made progressively more positive. For values of V_{coll} less than the bombarding voltage (V_{p1}) at which the external secondary emission yield σ of the target first attains a value of unity, the number of secondaries reaching the collector electrode will always be less than the number of primary electrons incident on the insulator. This will occur whatever the initial positive value of the insulator potential and the initial value of σ, since the collector cannot accept secondaries emitted with small

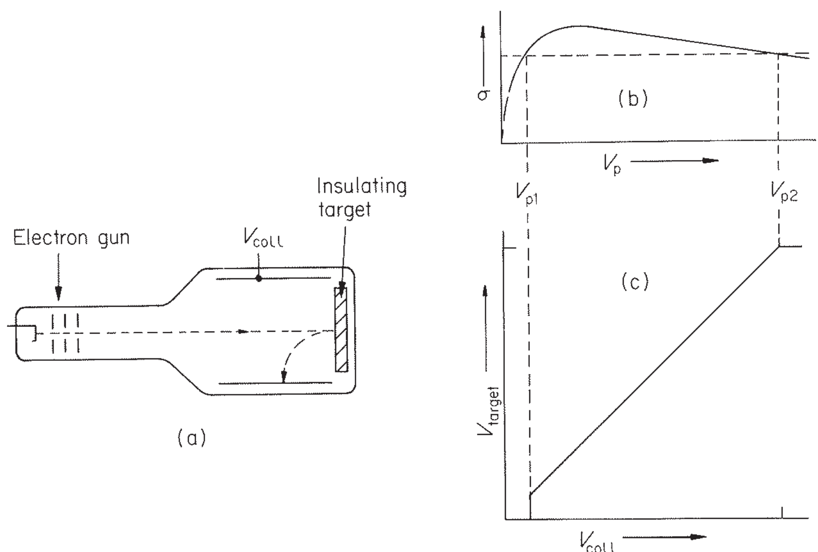

Figure 3.3. The stabilization potentials of an insulator when its free surface is bombarded by electrons. (a) Tube used to explain the text; (b) secondary emission yield curve; (c) surface potential of target as a function of collector potential. (Gibbons, 1966)

energies from a target at a potential more positive than V_{coll}. Thus the potential of the insulator will float in a negative direction until it attains cathode potential. This is known as cathode potential stabilization.

Qualitatively the shape of the secondary emission yield curve is shown in Fig. 3.3(b); this shape is representative of all materials. The potentials V_{p1} and V_{p2} are respectively the lower and upper target potentials for which σ has the value unity. Tables giving values of σ, V_{p1}, and V_{p2} for a number of materials are given in the Appendix.

As V_{coll} is increased beyond V_{p1} the target may remain at cathode potential but this is not the only stable state. Any increase of the target potential, even momentary, beyond V_{p1} will cause the emission of more secondaries than the number of primaries arriving, and the target potential will float positively. This potential will continue to rise until the target attains a potential slightly more positive than V_{coll}. Stabilization occurs at the potential where the number of primary electrons incident on the target is exactly balanced by the number of secondaries that can overcome the slight retarding field of the collector. This may be a few volts positive with respect to V_{coll}. This process is known as anode potential stabilization.

The target potential may now follow V_{coll} as it is increased until the higher potential (V_{p2}) at which σ attains a value of unity is reached. The target

potential can no longer follow to higher values because, beyond V_{p2}, the number of secondaries will always be less than the number of primaries and the target can only charge negatively. Thus, when V_{coll} is greater than V_{p2} the target potential will stabilize at V_{p2}. For this reason V_{p2} is often referred to as the sticking potential of the insulator.

These three stabilization conditions are shown diagrammatically in Fig. 3.3(c). In general, the condition of cathode potential stabilization can be achieved only if the stabilizing beam lands everywhere on the target orthogonally.

The free surface can be scanned by an electron beam in the form of a television raster. In this case a charge is induced in the back conducting contact if the beam replaces those charges that flowed through the insulator in the interval between scans. If the surface is stabilized at V_{coll} both positive and negative potential excursions can be discharged, but if at cathode potential ($V = 0$) only positive charges can be neutralized. The former method was used by Pensak (1949, 1950) to measure the EBC of thin insulating films. Diagrams of his apparatus are shown in Figs 3.4 and 3.5. His, or similar methods, have been used to measure the steady EBC of insulators in self-supported or weakly supported thin films.

There is good experimental evidence to support the belief that if an electron beam contact is used, and even if the contacting beam arrives at the specimen surface with such a low velocity that it can do little more than deposit a surface charge, it can act as an injecting contact for electrons. Thin films with either type of contact can be compared when it is known that the source material and deposition conditions were identical. Decker and Schneeberger (1957) measured films of As_2S_3 and found that values of EBC

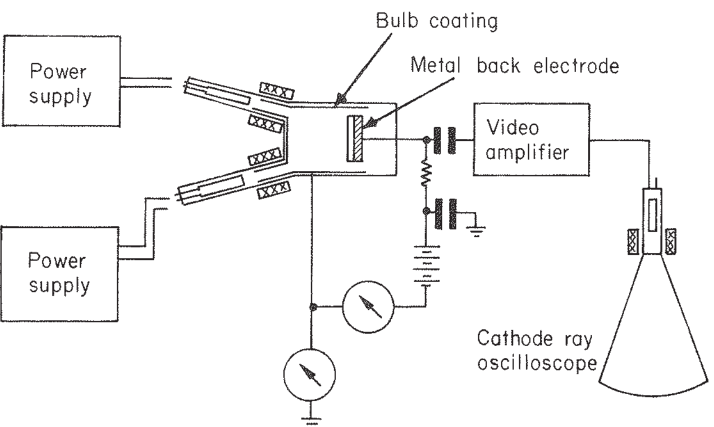

Figure 3.4. Experimental arrangement used to demonstrate the EBC of thin films of chemically deposited silica. (Pensak, 1949)

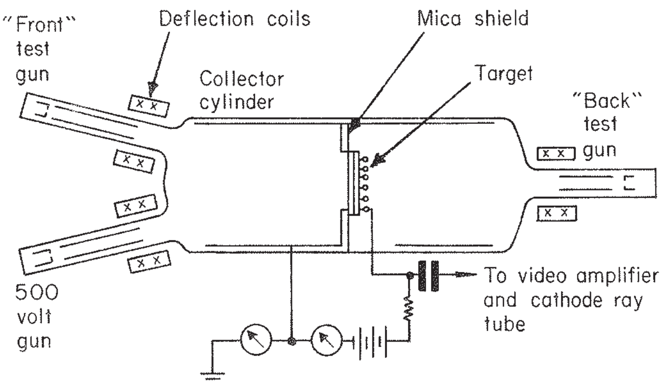

Figure 3.5. Experimental tube used to measure the steady-state EBC of lightly supported thin films of amorphous selenium when excited by electrons from either side. (Pensak, 1950)

gain when an electron beam was used were higher than those with a film having contacts of thin metallic layers. Bowman (1972) found similar behaviour for ZnS. This results in secondary EBC gain and it is thus accompanied by higher g values and increased very low-level conductance "tail", especially for long times after the end of excitation.

III. Transfer of excitation

A. X-rays

Firmin and Oatley (1955) first drew attention to the fact that when an insulator sandwiched between metallic electrodes is excited by electron bombardment (as in EBC) the influence of the excitation may greatly exceed the electron penetration depth. Since then, others have studied the influence of processes that could extend the depth of excitation, and the main results have been summarized by Bleil (1962) and Sturner and Bleil (1963).

The first experiment was performed on electron bombarded diamond crystals with thin silver electrodes of different thicknesses. The EBC was not measured directly, but the change in conductivity was inferred from measurements in which the specimen was placed in one arm of a Blumlein ac bridge (see Clark and Vanderlyn, 1949). This bridge uses closely coupled coils as ratio arms, and very high ratios of the measured capacitance to the known capacitance can be used. The change in the effective specimen series resistance Δr, or capacity ΔC, was used as a measure of the increased conductivity. It was found that the change in conductivity became greater as

the thickness of the top (bombarded) electrode was increased, provided that the beam energy exceeded a threshold. Firmin and Oatley further found that the value of Δr was 4 times greater for the same i_p and V_p if a piece of tungsten foil 1 μm thick was mounted in front of, but not touching, the diamond. This thickness of tungsten was enough to stop the 20 keV incident electrons so that none reached the specimen. It was inferred from this that X-rays generated in the front electrode seriously affected the excitation, because a small number of electron–hole pairs liberated throughout the bulk of the specimen would have had as big an effect as a much larger number generated directly near the surface. The greater range of X-rays compared with electrons has already been mentioned; this is more important if the specimen is too thick for the primary electrons to penetrate it completely.

The effect of X-rays was also studied in a detailed set of experiments on CdS by Bleil and his coworkers. Basically their experiment was to use two single-crystal specimens of CdS mounted in close proximity to each other. The two crystals were not quite touching, and they were optically screened from each other by a thin aluminium foil. The change in conductivity in both crystals was measured when only one of them was bombarded by electrons. It was shown that characteristic X-rays generated when electrons struck the Cd and the S atoms of the first crystal are capable of exciting conductivity in the other (non-bombarded) crystal. However, characteristic X-rays constitute only a small proportion of the total energy emitted. The total generation efficiency of X-rays by 50 keV electrons in CdS was calculated as 0·2% but the results showed that only a small part (of the order of 10^{-5}) of the energy available in the X-rays was needed to explain the observed changes in conductivity.

The experiment of Firmin and Oatley was repeated with a copper foil a few tenths of a mm thick in a series of experiments with CdS using beam voltages up to 90 kV. As expected, the role of X-rays in producing a change in conductivity was confirmed.

It was subsequently found that the role of some specific X-rays, such as the characteristic rays emitted from the constituent atoms, is more pronounced in CdSe than in CdS. In particular, the importance of the double conversion electron–X-ray–electron was found to be significant and that the importance of individual characteristic X-ray wavelengths due to Cd_K and Se_K can be clearly demonstrated (Sturner and Bleil, 1963).

B. Excitons

If the primary electrons generate excitons or electrons and holes which diffuse through the lattice by ambipolar processes, energy can be deposited

at distances from the point of entry many times the penetration depth of the beam. The energy carried by the primary beam may thus be spread by mechanisms of this kind. In organic or molecular crystals there is also migration of molecular excitons—the equivalents of excited states of isolated molecules. In any of these cases, energy is transported without the net movement of charge, and energy is liberated in the form of a phonon or a number of phonons when the electron and hole recombine or, in the case of the molecular exciton, when it reverts to its ground state. The localized region of high phonon density can now lose its energy either by liberating electron–hole pairs or by diffusing through the lattice.

Exciton diffusion in CdS crystals when they were illuminated by light at some distance remote from the electrodes was studied extensively; the same considerations would apply of course in the case of EBC. Large values of the diffusion length were shown to be due to excitons, by a combination of measurements involving the spectral response of photoconductivity, the temperature dependence of the diffusion length, and the PEM voltage. A thermal activation energy of about 0·1 eV was found for exciton migration in CdS, and diffusion lengths ranging from a fraction of a μm to several hundred μm were observed (Diemer and Hoogenstraaten, 1957; Diemer *et al.*, 1958). Using these results and others, Bleil assigned an exciton diffusion length of 0·4 mm to his CdS crystals excited by electrons, and an ambipolar diffusion length of 1 μm or less. This compares with a mean attenuation length of about 1 cm for X-rays of 10 keV energy in a typical crystal.

One of the most extensively studied organic crystals is anthracene. In this material, singlet excitons were found to have a diffusion length of about 1000 Å but there is a complication in the mechanism of energy transfer. The singlet exciton may undergo what is termed inter-system crossing, by changing from the excitonic structure corresponding to the singlet excited states of the molecule to that corresponding to the triplet states. The triplet exciton has a much longer life and hence a longer diffusion time. In anthracene its lifetime is typically 6 ms and the diffusion length can be as long as 2 μm. The excitons decay to their ground state and, with the assistance of a small amount of additional energy from collision with a surface state or an impurity, free carriers may be produced.

Thus, in the particular case of some molecular crystals where the lifetime of triplet excitons is long, this mechanism of energy transfer is often accompanied by a process of delayed generation.

C. Fluorescence

A solid such as CdS, which can be fluorescent as well as photoconductive, is capable of exhibiting the influence of excitation by an electron beam at some

distance from the point of measurement owing to its own light emission and absorption. This was studied by Diemer *et al.* (1958) who concluded that, for separations greater than about 4 mm, the visible light fluorescence of a copper-activated CdS sample could be responsible for 80% of the change in conductivity. Taking into account the accuracy of the measurements, they concluded that exciton diffusion did not play a measurable part at this distance in the crystal they used.

However, an interesting and unexplained effect was discovered. It was found that infrared light ($\lambda \approx 850$ nm) was effective in quenching photoconduction. This might have been expected, since they were observing secondary photocurrents, but they found that, if infrared light was allowed to fall on part of the crystal containing the electrodes while a nearby region was illuminated by a narrow patch of green light, the quenching effect was about 10 times greater than when that region of the electrodes was illuminated directly. The authors suggested that the occupancy of the centres with which the excitons interact giving rise to photoconduction might be changed by the infrared light.

A different situation applies to organic rigid glasses and to plastics (Förster, 1959). In these a process called resonance transfer can take place; this has the same basic requirements as radiative transfer just discussed for CdS in so far as the absorption spectrum of the accepting molecule overlaps the fluorescence spectrum of the emitting molecule. Normally, in the isolated molecule, Stokes's law states that the absorption peak is at a shorter wavelength than that of the fluorescence. However, in condensed phases, neighbour interactions will broaden the spectral line widths, and overlap is more likely. In the case of resonance transfer, no emission or absorption of photons takes place. Dipole–dipole interaction between neighbouring molecules is mainly responsible for direct coupling of the mutual radiation field of two excited molecules. In practice, the resonance condition is usually soon broken because the accepting molecule loses thermal energy to the lattice as soon as it receives enough energy to raise it to an excited state. Further diffusion therefore stops and the excited molecule now decays to its ground state. This process may transfer energy over a range of only 5–100 Å.

IV. Conductivity induced by electrons

The conductivity of films measured through their thickness is many orders of magnitude greater than that in their plane. Since 1948 conductivity changes under electron bombardment have been studied in a variety of insulators that might be highly resistive in the absence of bombardment.

A. Influence of bombarding voltage

1. The threshold

When a space-charge-free film of a typical insulating solid appropriately biased by an applied voltage across its thickness is exposed to a short burst of electrons, a charge due to internally generated carriers is induced on the electrodes. We then define the gain as the ratio of this charge to the bombarding charge. On repeating the excitation the gain decreases and finally vanishes unless the energy qV_p of the impinging electrons exceeds a threshold qV_0. As a result, the response to *steady* bombardment commences only at electron energies above qV_0. The gain then rises to a maximum g_m at $V_m \approx 2V_0$ beyond which it declines because the electron energy lost in the film decreases. The gain above the threshold increases with bias but is normally not more than about 100. Figure 3.6 shows a typical family of curves giving the EBC gain (g) of a thin film of amorphous As_2S_3 as a function of bombarding voltage (V_p), with applied bias (v) as a parameter. It is seen that, even at 105 V bias, about 1000 eV are dissipated at V_m for each

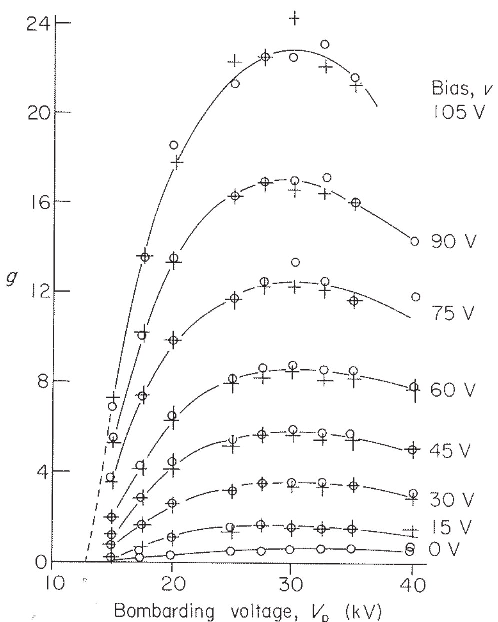

Figure 3.6. The EBC gain g of a thin film of amorphous As_2S_3 as a function of electron bombarding voltage V_p, with applied bias voltage v as a parameter (O negative gain; + positive gain). The shape of these curves is typical of those for all amorphous insulating thin films in which there is no carrier injection from the electrodes. (Ansbacher and Ehrenberg, 1951)

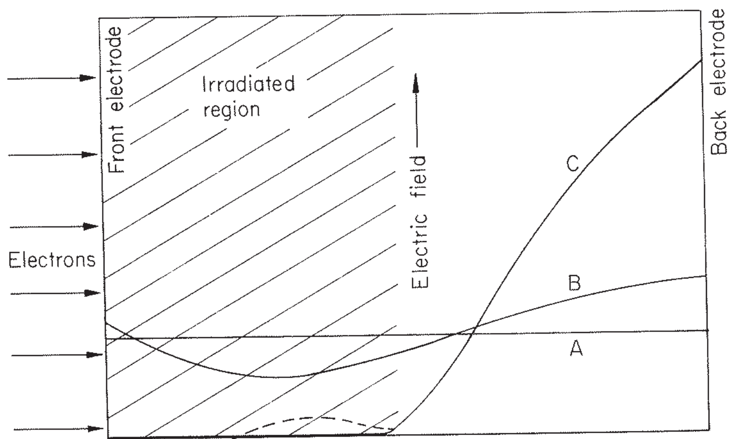

Figure 3.7. Schematic representation of the electric field in a dielectric bombarded by electrons that do not penetrate the slab; the left electrode is positive. A, before bombardment; B, after a brief pulse of electrons; C, equilibrium under steady electron bombardment. The broken line refers to the case where the positive carriers are less mobile than the negative carriers. (Ehrenberg and Hidden, 1962)

carrier moved across the film. The threshold, and V_m with it, moves to higher voltages as the thickness of the film increases.

The behaviour at low electron energies has been explained on the basis of the presence of a very large number of traps with escape times long compared with the intervals between the bursts of excitation. Figure 3.7 shows an insulating lamina fitted with thin front and back electrodes. Of the carriers generated near the front electrode, those with the polarity of this electrode are pulled out of the plasma and may be trapped in the non-irradiated regions shown on the right-hand side of the diagram. The process continues until the charge in this region is so large that it takes up the whole potential drop across the specimen. This progressive change is shown by the sequence of potential curves: A, initial distribution uniform; B, slight space charge build-up; C, final stable potential. The plasma region then becomes field-free and carriers are no longer encouraged to leave it, and recombination in the generation region becomes severe. Since the threshold applies equally to positive and to negative carriers it must be concluded that both are mobile and liable to be trapped. In the non-irradiated region no recombination can take place; after delays depending on the depths of the traps, the carriers will eventually again become mobile.

The existence of a threshold is typical for amorphous films but not displayed by all films. A number of experiments have been carried out in order to examine the nature of this threshold. Ansbacher and Ehrenberg (1951) measured the charge trapped in an As_2S_3 film bombarded with electrons

having energy near the threshold by interrupting the bombardment when the induced current had dropped to zero. After reducing the bias to zero they connected the electrode through a ballistic galvanometer; the stored charge is discharged on renewed bombardment. On a specimen 2 μm thick of As_2S_3, $1{\cdot}4 \times 10^{-7}$ C cm^{-2} was discharged; this would have caused a field of about 2×10^5 V cm^{-1} (taking the dielectric constant of the material as 7). Even if this charge is distributed over half the film, it requires 10^{16} traps cm^{-3}; this estimate is a lower limit but it is within the range commonly found for amorphous solids.

An estimate of the density of filled traps can also be obtained directly from the bias at which the threshold is observed. Thus, Ehrenberg and Hidden (1962) gave a lower limit of 10^{18} cm^{-3} for evaporated ZnS films, assuming that the filled traps occupy half the specimen. A similar consideration led these authors to an estimate of the energy required to create a mobile pair. The dose, at an energy near qV_0, was measured after the response had been reduced to half that of a virgin film. Since the gain is proportional to the bias for ZnS films, the charge must then cancel half the applied bias. This was found to correspond to the creation of one mobile pair for each 2000 eV dissipated by the beam.

On his silica films Pensak had observed a rapid decline of the conduction effect with decreasing bombarding voltage, and had suggested that it occurs when the penetration ceases to be complete. Ansbacher and Ehrenberg also interpreted the threshold as the beginning of complete penetration of the specimen by fast electrons. Spear (1955), examining transmission and EBC on the same specimens, found however that electrons commence to be transmitted only when their energy reaches qV_m, and that the range of the bombarding electrons at the threshold is about half the specimen thickness. This was confirmed by Bowlt and Ehrenberg (1969), directly and by comparison with Spencer's electron range calculations.

All experiments have confirmed that the threshold effect is related to the build-up of space charge although details of the process are still obscure. It is not explained why sufficient space charge to compensate the applied bias occupies half the specimen, so that for example 1 μm is sufficient in a 2 μm specimen but insufficient in a 4 μm specimen.

The response to a pulse can be taken as a measure of the existing space charge; for example, a steady response indicates that the space charge has reached its limiting value for the particular bombarding conditions. This state was first established in a series of experiments carried out by Bowlt and Ehrenberg (1969), illustrated in Fig. 3.8. The top surface of a self-supporting film of As_2S_3 was bombarded with electrons; the controlling space charge was then expected to reside in the lower portion of the film. Then the specimen was bombarded from the bottom at zero bias in order to

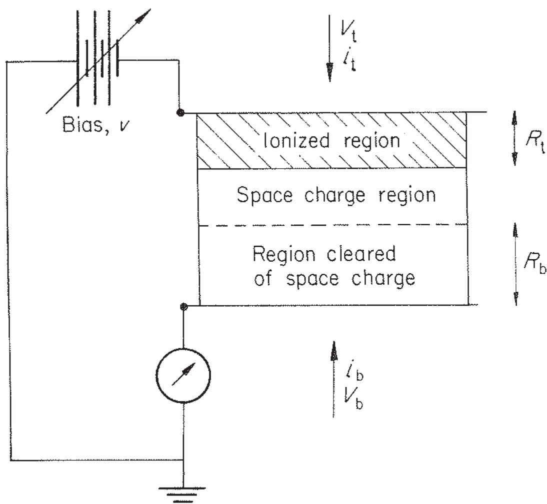

Figure 3.8. The two-beam experiment. Schematic diagram of the ionized region and the space charge region produced by top bombardment, with an applied bias; the region cleared of space charge by bottom irradiation is also indicated, and R_t and R_b are the practical ranges of bombarding electrons from the top and from the bottom respectively. (Bowlt and Ehrenberg, 1969)

remove the space charge in a region adjoining the bottom surface; this created a strong ionization in which the trapped carriers were liberated and conducted away through the bottom electrode. A strip of space charge remained intact in the middle region, unless the cathode rays from the bottom reached the plane at which the rays from the top had stopped. In the third stage of the experiment, the response to a single shot from the top was measured at the original bias and electron energy. It indicated how much of the space charge established in the first stage was left; it would have been equal to the response of a virgin specimen if the space charge had been completely removed.

Results for an arsenic trisulphide film with a threshold of 23 kV are shown in Fig. 3.9. The sensitivity of the method is limited to the cases where the space charge decay in the interval between first and second stages mentioned above is less than the irradiation induced clearing. The natural decay accounts for the larger than steady-state gains at low values of the bottom bombarding voltage and especially in the absence of irradiation from the bottom.

In the second curve the pulses of electrons from the top have an energy of 23 keV which is the threshold energy for this film. It is seen that a small effect is observed even at $V_b = 10$ kV, but that it requires electrons of about nearly threshold energy impinging on the opposite side to restore the full response.

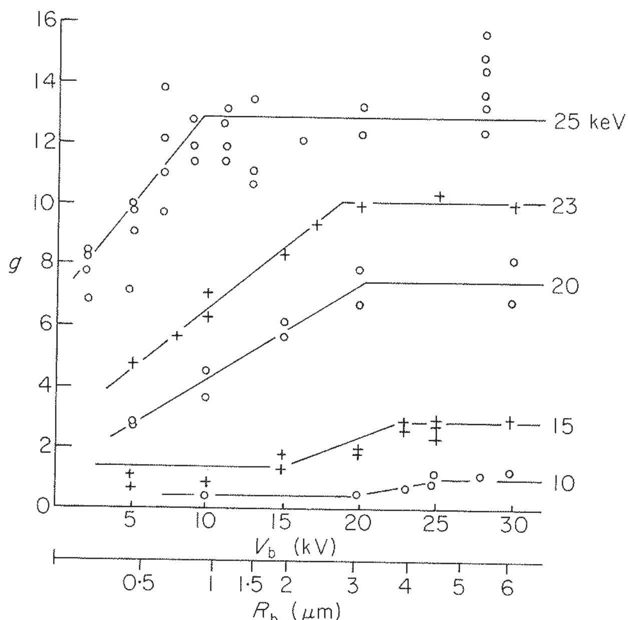

Figure 3.9. Induced conductance gain of the first pulse of fast electrons from the top gun at various energies. The pulses of electrons from the top gun (V_t) were interrupted by irradiating the specimen with electrons from the bottom gun (V_b). The lower scale gives the penetration depth (R_b) of the electrons. a-As_2S_3 film thickness 6·6 μm; $i_t = 5 \times 10^{-9}$ A (pulsed); bias $v = 200$ V (top negative). (Bowlt and Ehrenberg, 1969)

Thus, as V_b (and hence the penetration of the neutralizing beam) increases, more and more of the space charge is swept away until at $V_b = V_{b2} = 20$ kV the whole space charge layer is neutralized and g ceases to increase. The limits of penetration R_t and R_{b2} of the 23 kV and 20 kV electrons are 3·9 and 3·1 μm respectively; the sum is 7 μm, slightly more than the thickness of the film. The results show that the space charge extends from about the middle of the film, i.e. the end of the range of the bombarding electrons, to very near the bottom electrode.

At higher V_t (top curve) the space charge layer commences nearer to the bottom of the film, so the neutralizing electrons have to penetrate less deeply in order to release all the space charge. But for $V_t = 15$ kV and 10 kV (third and fourth curves) the irradiation induced clearing of the space charge is small or absent when the penetration of the bottom electrons is small. Accurate measurements are therefore difficult in this region but the results suggest that at low values of V_t very little charge resides near the bottom electrode. The difference ($R_{b2} - R_{b1}$) of the penetration depths at which the upward trend of the curves commences and ends (indicating clearing of the

space charge) showed that the thickness of the space charge layer ($R_t + R_{b2}$) should equal the thickness of the film. This was indeed found to be the case, within a reasonable margin of error.

In another series of experiments a specimen was exposed to repetitive bursts of bombardment on one side or on both sides. With As_2S_3 2·6 μm thick, at 100 volts bias, gains of 80 and 25 were observed at $V_p = 18$ and 13 kV respectively (ranges 2·6 and 1·5 μm) when one side only was bombarded. The same gains were recorded for 12·7 and 9·2 kV respectively (ranges 1·3 and 0·8 μm) when both sides were bombarded. This shows that the gain depends on the sum of the ranges, and has its full value when the formation of a space charge is prevented. Top and bottom pulses need not be exactly simultaneous. Second only to As_2S_3 among insulating films, ZnS has received the most attention. Tests have been made on glass-supported sandwich films (Ehrenberg and Hidden, 1962; Benoit *et al.*, 1969) and on lightly supported films (Didenko *et al.*, 1959; Guillard and Charles, 1966; Bowman, 1972) which were stabilized on one side by a low velocity scanned electron beam. Didenko *et al.* exposed this non-metallized side to both the "writing" gun and the stabilizing gun, operating at a voltage causing high secondary emission, whereas Guillard and Charles, and Bowman, let the "writing" gun operate from the supported metallized side of the film, and stabilized the other side by a beam of nearly zero velocity electrons.

The experimentalists who examined glass-based films found clearly marked thresholds and gain values between 10 and several hundred. Benoit *et al.* found that X-ray diffraction photographs indicated very disordered lattices which could be improved by annealing at elevated temperatures; initially the films might have been amorphous. Didenko *et al.*, on the other hand, kept their mica-Al bases at 120–150°C *during deposition* and reported gains of up to 360 but no clear threshold. Diagrams given by Guillard and Charles indicate similar gains and also the absence of a threshold. The targets examined by Bowman fall into two groups, giving gains of up to about 500 and of more than 1000 respectively; only the former displayed a well defined threshold. Figures 3.10 and 3.11 summarize Bowman's results. One explanation of this behaviour is that ZnS, quite different from As_2S_3, is very easy to crystallize but tends to have disordered lattices with an interplay between the wurtzite and the blende form. It is therefore reasonable to associate the differences in EBC behaviour with different degrees of crystalline perfection, which is completely lost in the amorphous form. Ehrenberg and Hidden had found that thin crystal platelets gave gains without threshold that were about 1000 times higher than those given by amorphous films deposited from the same material.

The idea that the existence of a threshold is due to the super-abundance of traps in the amorphous state is confirmed by experiments carried out by Bril

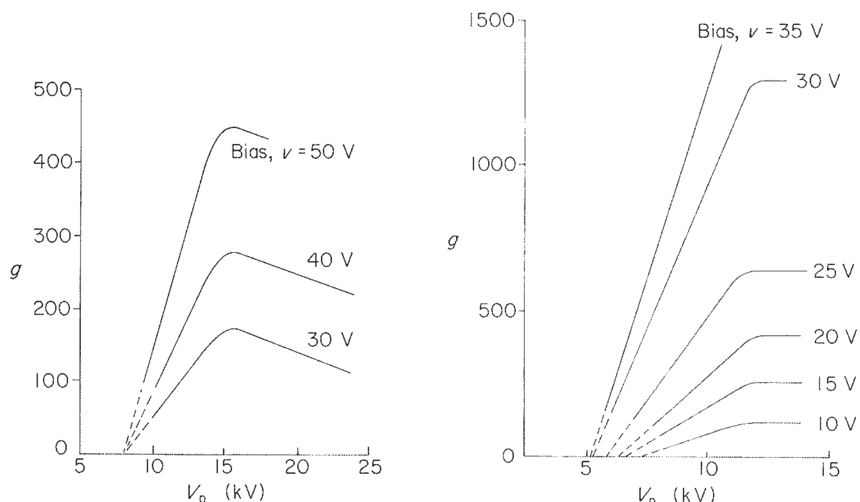

Figures 3.10 and 3.11. The steady EBC gain of thin lightly supported films of ZnS with an electron beam contact on one side. (Bowman, 1972) LEFT "low gain" film; RIGHT "high gain" film.

and Gelling (1962) who examined layers of cadmium selenide 5–25 μm thick sandwiched between glass (made conductive by a coating of tin oxide) and a thin film of aluminium. The film was bombarded through the aluminium with electrons of 10, 15, and 20 keV energy. The authors estimate that 20 keV electrons penetrate only 2 μm. In spite of this, a steady gain of about 2000 was observed in a film 15 μm thick, at a negative bias of 20 volts. The interesting point is that the temperature of the substrate during evaporation has a decisive influence on the structure of the evaporated layer; the higher the temperature the greater the opportunity for the condensing material to arrange itself into a neatly crystalline solid. The authors also report that the gains of their films, and their dark resistance, were appreciably enhanced when the films after deposition were exposed to copper vapour so as to give them a Cu content of 0·1 mol%, and heated at about 400°C in the presence of sulphur vapour to compensate for any excess Cd. The holes were found to be immobile, so the steady current must have been maintained by injection; this is confirmed by the rapid increase of gain with bias.

Selenium evaporated in a vacuum is deposited in the red amorphous modification. Pensak (1950) found that the gain of these films is exceptionally large and that considerable currents are induced with positive bias at less than 2 keV electron energy in films 1 μm thick. This means that there is no threshold. These results were confirmed by Spear (1956) who also found that, for low bombarding energies and currents, the induced current satu-

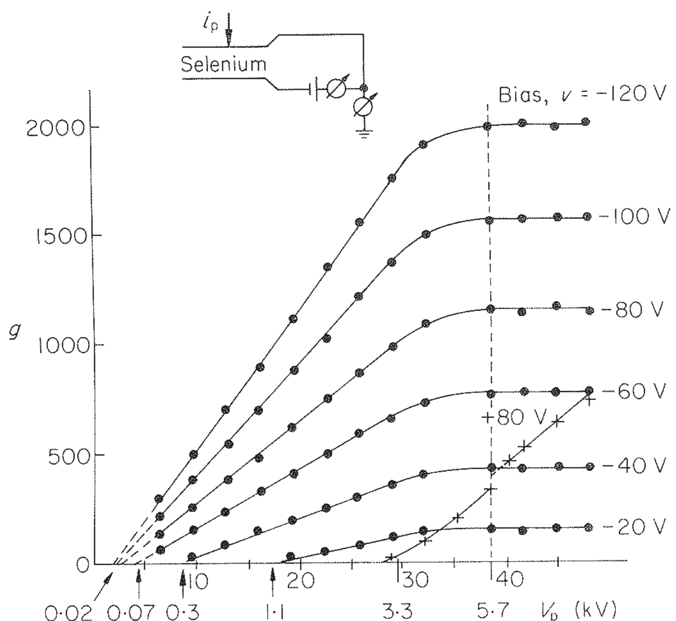

Figure 3.12. Amorphous selenium. Graph of gain g as a function of bombarding voltage V_p, for different values of applied bias v; $i_p = 1{\cdot}4 \times 10^{-8}$ A, specimen thickness 5·7 μm. Numbers below the V_p axis are calculated values of the average penetration depth of the bombarding electrons in μm. (Spear, 1956)

rates with bias when an average of about 20 eV energy is used for the creation of a pair (see Fig. 3.12).

Broerse (1966) produced polycrystalline films of PbO about 3 μm thick that were highly photosensitive and cathode ray sensitive by evaporating the material in the presence of oxygen; the density of these films was about half that of the bulk material. There was no threshold; the gain increased linearly with bias initially and then appeared to saturate above 50 volts bias at about $g = 100$ with 10 keV electrons and $g = 700$ with 20 keV electrons.

2. *The maximum*

If there is no entry of carriers from the electrodes (i.e. "primary" EBC), as the energy of the primary beam is increased, the gain increases rapidly and comes to a maximum (g_m) at about twice the bombarding energy of the threshold. At qV_m the ionization of the specimen is roughly uniform, and the gain varies only slowly with electron energy. Spencer's calculations show that, at qV_m, about half of the energy of the electrons entering the platelet is dissipated in it (i.e. the energy of the impinging electrons less the energy of those back-reflected). It is common for qV_m to be chosen as the energy for EBC studies of films.

At $V_p = V_m$ the induced current should be the same for either polarity of bias, neglecting the charge carried by the cathode rays. This is not always exactly the case, perhaps because the ionization is not strictly uniform, and the two surfaces are not quite equal. The existence of a maximum and its variations with film thickness were first reported by Pensak (1948) who observed gains of up to 70 for very thin films of silica deposited on Nichrome plates by thermal decomposition of ethyl silicate vapour, at the highest bias the films would tolerate. For aluminium oxide, values of g up to 15 have been reported (Ansbacher and Ehrenberg, 1951), for As_2S_3 values up to 60, and for Sb_2S_3 higher values. Sb_2S_3 was also examined in more detail by Oksman and Tikhomirov (1959) who used films deposited on thin metallized organic foils and stabilized on the other side by secondary emission; the much higher gain (up to 600) found by these authors is probably related to the difference in measuring techniques.

All such figures are of course of restricted significance. They do not take into account the increase of gain at elevated temperatures, the injection of carriers, the effect of thickness, etc. It would therefore serve no useful purpose to compile and present a list of observed gains.

3. *Space charges in the steady state*

Ansbacher and Ehrenberg (1951) suggested that, for uniform ionization, Thomson's and Mie's idea of the ionization chamber should apply, thus allowing for carriers firmly trapped near the electrodes. In the central region of the specimen the applied field is then reduced by the charges near the electrodes. Following Newton's (1949) analysis of McKay's (1948) work on diamond, which showed that the electric field in the centre of the specimen was less than about 200 V cm^{-1}, Ansbacher and Ehrenberg related the gain at $V_p = V_m$ to the mobility (μ) of the carriers, idealizing the field as having one value in the two boundary regions and another in the central region. A mobility of 6×10^{-4} cm^2 V^{-1} s^{-1} was suggested. Alcock (1962) and Ghosh (1967) attempted to estimate the charges stored near the electrodes for As_2S_3 and Spectrosil films (SiO_2) as follows. After exposure to electrons at $V_p = V_m$, at given applied bias, the bombardment was interrupted and, after a short interval, re-started with zero bias. The field due to the charges near the electrodes then provides a bias which caused an induced current to flow in the opposite direction. The initial current depended on the interval, but its value at zero interval was found by extrapolation. The bias responsible for this current was found to increase with the charging current but never to

exceed 10–20% of the bias at which the specimen was charged—a percentage low enough to justify the procedure. Ghosh pointed out that a reverse current is observed after the bias has been reduced to zero on As_2S_3 film even without renewed bombardment. This reverse current must be allowed for when estimating the effective bias. The curves given show that in the absence of irradiation the charge decays initially to $1/e$ in about 30 s, and to $1/e^2$ in about 100 s. Gibbons (1974a) studied the stored charge by recording the discharge current on successive bursts, after the removal of the bias, in thin films of As_2S_3 and ZnS. It was found that substantial discharging currents could be detected and that, with successive pulses of electron excitation under a finite forward or reverse bias, the amount of trapped charge reached a saturation value. The size of the discharge pulse under zero bias is shown in Fig. 3.13 as a function of the number of equal duration excitation pulses.

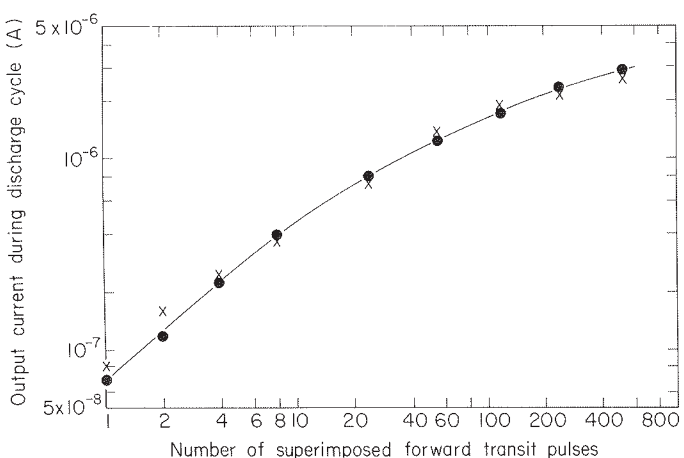

Figure 3.13. Discharge pulse amplitude as a function of the number of superimposed equal forward induced current pulses (● positive bias, X negative bias; discharge bias zero). Zinc sulphide evaporated film 0·9 μm thick, V_p = 14 kV. (Gibbons, 1974a)

The amplitude of the discharging pulse could be fitted to a Hecht curve from which values of the schubweg (w)could be deduced. Values of w/bias field were found to be of the order of 10^{-13} m^2 V^{-1} for evaporated ZnS. The deduced values of w ranged from 0·08 to 3·1 μm for specimens in the thickness range 0·4–2·0 μm.

It is worth noting that in these charge storage experiments the EBC effect is responsible for both charging and discharging the specimen, according to the value of the bias. With the open film technique (Pensak's method), in particular with ZnS films, a different kind of charge storage has often been employed and has become of technical importance. The film acts as the

dielectric in condenser elements of which the electrodes are the free surface and the metal backing. Areas of the surface are charged by scanning it with an electron beam which stabilizes it by secondary emission at the potential of a neighbouring grid. Electrons from a different source and of higher energy make the dielectric leaky so that the condensers are discharged; the charge required to bring the surface back to its original value is then a measure either of the gain at given current density or of the density and duration of the cathode ray current at given gain.

4. Secondary EBC

Secondary EBC gain can be explained by reasoning analogous to that used in the case of secondary photoconductivity, but it should be emphasized that the word "gain" has slightly different meanings. In EBC, gain is the ratio of circulating current to bombarding current; in photoconductivity, gain is the ratio of the number of circulating charge carriers to the number of incident photons. The secondary effect in photoconduction arises through one sign of charge carrier being trapped near an injecting electrode which thereby increases the electric field in its vicinity and enhances injection. These trapping centres are known as activation centres; they have a high trapping cross-section for one sign of carrier and thereafter a low recombination cross-section for carriers of the opposite sign. If t' is the carrier lifetime in the presence of filled activation centres, and T is the transit time, the secondary photoconductive gain is given by $G = t'/T$. In EBC the explanation of the secondary effect is similar; the secondary EBC gain is given by $g' = gG$, where g is the EBC gain for the primary effect.

Activation centres can be introduced into CdS, CdSe, or ZnS by adding impurities such as copper or silver. Secondary EBC gain values in the region of several thousand at room temperature can be observed in stoicheiometric and non-stoicheiometric formulations of Se–S, Se–O, Se–O–S, Se–Cd–S, As–Se–S, Cd–As–S, and Zn–Cd–S. Secondary gains up to 40 000 have been seen for As_2S_3 at high temperatures; they can be up to 2000 for amorphous selenium at room temperature and as high as 10^{10} for single crystals of CdS activated with copper and chlorine. Secondary gain is always associated with time lag effects, and usually the higher its value the longer the response time. The cited targets having g' values in the region of 1000 had a response time of about 1 s, and the very high gain of 10^{10} was measured on a CdS target with a time constant of many minutes.

B. Gain

The gain at qV_m, at a bias just below breakdown, is a measure of the EBC sensitivity of the material. Normally materials with large gains are also

photoconductive in some region of the spectrum. If the gain is of the order of unity or even less, of course it matters whether its definition does or does not include film leakage (i_l) and the primary current (i_p). In these cases gain must be defined as either

$$g = i_s/i_p \quad \text{or} \quad g = (i_c - i_b - i_l)/i_p$$

where i_s is the secondary (induced) current, i_c is the total conduction current, and i_b is the current due to primary electrons reaching the bottom electrode. In practice i_b can be measured by determining the current flowing in the circuit containing the specimen when the bias is reduced to zero.

1. Gain as a function of thickness

Observations on specimens having different thicknesses have supplied valuable evidence as to how the applied bias increases the EBC gain in thin films. However, there is uncertainty about such results because even values for gain measured on equally thick samples often vary by perhaps 30% or more if the technique for preparing them is not rigorously controlled. Pensak (1949), comparing films of silica between 0·25 and 1·5 μm thick, found that the gain at V_m is approximately proportional to the energy dissipated. In the light of Hecht's formula, this suggests that the schubweg of the carriers in these films is much longer than 1·5 μm. However, this was not Pensak's conclusion; he was puzzled as to how his results could be reconciled with a gain much smaller than the ratio of qV_m and the band gap. Ghosh (1967) and Ehrenberg and Ghosh (1969) also found that the gain for As_2S_3 between 2 and 6 μm thick was proportional to V_m. At a field of 10^5 V cm^{-1} the corresponding value of the mobilization energy E was 650 eV. An independent series of samples led to the same result, and a third series gave $E = 215$ eV with a field of 2×10^5 V cm^{-1}. The calculated schubweg varied considerably, from 6 to 50 μm, but was never small compared with the sample thickness.

These authors also examined films up to 22 μm thick excited by β-rays from a Sr-90 (+ Y-90) source. Under this excitation the gain reached its final value only after 2 hours, when it was 2–3 times greater than after 30 s. Although the thickness fitted the Hecht pattern reasonably well, the schubweg was only 1–2 μm after 30 s with $E = 54$ eV at a field of 10^5 V cm^{-1}; after 2 hours the schubweg was even shorter and the mobilization energy had fallen to 1·8 eV at 3×10^5 V cm^{-1}.

At first sight it might appear that the mobilization energy is much greater than the radiant ionization energy on account of Shockley–Read recombination. But the electron bombardment results pretty well exclude the possibility that this alone is responsible for such a large discrepancy; it could be due to initial or columnar recombination—or both. The authors decided that

columnar recombination was mainly responsible because of the higher value of E for cathode rays than for β-rays, the density of ionization along a track being much greater for cathode rays than for β-rays. Some later results of Ing *et al.* (1971), who found the photoconductive quantum efficiency of As_2S_3 films to be of the order of unity for blue light at fields in the neighbourhood of 10^6 V cm^{-1}, also suggest that initial recombination plays only a minor role. The initial recombination for photons can barely be smaller than that for cathode rays.

The different values for β-rays were attributed to their tracks being straight and parallel to the field, so the carriers moved in the wake of the tracks. This interpretation does not explain the apparent reduction of the schubweg with increasing exposure. A high rate of injection of carriers caused by a slow build-up of the field near the electrodes would make the gain just as independent of the thickness of the specimen as would a short schubweg.

Recombination of carriers explains in general why the gain does not come up to expectations. However, on As_2S_3 films at high values of bias (and especially at elevated temperatures) the gain rises above the value that could not reasonably be expected without any tendency to saturate. This effect has been related to the injection of carriers from the electrodes, and no other explanation seems to be possible.

Mott and Gurney (1940) first drew attention to the possibility that the work function of the electrode material with respect to a dielectric can be so small that a significant cloud of electrons exists in equilibrium in the dielectric near the electrode. An electric field will draw this cloud to the opposite electrode. Mott termed this effect space charge limited current. The effect here referred to is of a similar kind.

Trapping of carriers near the electrode can increase the average field acting near it by a factor of the order of 10, and more due to statistical fluctuations. In the experiments, fields up to 10^6 V cm^{-1} are applied. Field emission rises according to the Fowler–Nordheim formula from 10^{-11} to 10^{-9} A cm^{-2} when the field increases from 10^6 to 3×10^6 V cm^{-1}. Carrier injection is therefore a predictable effect. Because gain rises with bias owing to reduced recombination and because of rising or falling injection of carriers, any region of saturation must be expected to be masked.

2. Gain as a function of applied field

The current induced in films always increases with bias. Of course, even the best films break down at fields of about 10^6 V cm^{-1}, but experimental evidence suggests that the absence of saturation is not due to weakness of the field.

At moderate fields the gains are so low that no tendency to saturate could be expected; they have been shown to be only a small percentage of what is energetically possible. It is seen from diagrams such as Fig. 3.6 that, as a function of V_p, the gains recorded for different values of bias have the same shape and can be made to coincide by multiplying them by a factor $f(v)$. Ansbacher and Ehrenberg (1951) found that gain increases linearly with bias at low temperatures and becomes quadratic in bias as the temperature increases. They provided a curve showing the gain at fields between 5×10^4 and 6×10^5 V cm^{-1} for various specimens of As_2S_3 film; it increases in this range from 1 to 40. Ghosh found that, at room temperature over a wide range of bombarding currents and specimen thicknesses, the gain for As_2S_3 films is proportional to $v^{1 \cdot 4}$; for Spectrosil and fused quartz the gain is proportional to $v^{1 \cdot 25}$. For sandwiched ZnS films, Ehrenberg and Hidden found that the gain was proportional to the bias. Benoit's curves indicate a superlinear increase. For open ZnS films Didenko *et al.* and Bowman found that the induced current can be represented as a power of the bias, with an index not exceeding 2. Guillard and Charles claimed an exponential increase of gain with bias for their open films, but this was based on a rather small range of values.

We have to ask why the bias influences the generation or recombination of carriers so that only a minority of them contribute to the circulating current. In order to recombine, a carrier must find another carrier of opposite sign; it can normally do this in an insulator only within the plasma. The longer the carriers remain in the plasma the greater is their chance to recombine—whether the plasma is restricted to a thin layer near the bombarded electrode or extends over the whole film. We would therefore expect the fraction of carriers escaping recombination and contributing to the gain to be greater the higher the drift velocity of the more mobile carriers. Hence the gain should be proportional to the bias if it is small, and a measure of mobility and trap density.

In the scheme referred to as Shockley–Read recombination, two stages are involved, the creation of a pair by the incident radiation, one partner of which is either initially localized or becomes localized after some diffusion. If now a mobile charge of opposite sign (one of a pair created elsewhere) comes near to this localized charge, it can neutralize it so that, of two mobile pairs, one has disappeared. In the first process a carrier is trapped and hence can become free again. Only the second event terminates the career of a carrier.

In order to gauge the effect of recombination on the circulating current, Hecht (1932), studying field dependence in photoconductivity, introduced the concept of schubweg (w). This is the mean distance a carrier travels in the direction of the field before it recombines or becomes trapped. If the specimen is L units thick, the carrier contributes the charge $(w/L)q$ to the charge measured in the external circuit. The actual path of the carrier is devious and much longer than w, because the field has only a slight effect on the carrier's movements. As a result, w is proportional to the field. If $w \ll L$, and the ionization is uniform, the gain will be w/L times the number n of carriers set free per primary electron, and hence proportional to the bias and independent of the thickness of the specimen. If $w \gg L$, each carrier pair will contribute the charge q and $g = n$; the gain is proportional to the energy lost by the incident electrons, i.e. to V_m if the electron is re-adjusted to V_m for varying thickness. Hecht's formula for intermediate cases will be referred to in Chapter 5.

A carrier released by radiation can also disappear by initial recombination, i.e. by returning to its parent atom. This can happen because it loses the kinetic energy with which it is ejected by collision and can be left with only thermal energy while still within the range of Coulomb attraction. If it is far enough, of course, the bias field will prevent the return. The distance from the parent atom at which the applied field can be equal and opposite to the Coulomb attraction is, neglecting screening, given by $q^2/r^2 = q\mathscr{E}$ or $r = \sqrt{(q/\mathscr{E})}$. For $\mathscr{E} = 10^5$ V cm^{-1}, $r \approx 1 \cdot 3 \times 10^{-6}$ cm ($q = 1 \cdot 6 \times 10^{-19}$ C). This distance is of the same order as that at which a carrier is normally expected to have become thermalized. Onsager (1938) estimated the effect of a bias field on initial recombination; fields of 10^4, 10^5, and 10^6 V cm^{-1} will reduce the probability by 1/2, 1/10, and 1/100 respectively.

Columnar recombination stands between initial recombination and recombination in Shockley–Read centres.

It was Langevin (see Moulin, 1908) who first drew attention to the special nature of the ionization by α-particles, viz. the high linear density of ion pairs along the track (columnar ionization) which must greatly increase the rate of recombination and the field necessary for saturation. A detailed experimental study by Moulin fully confirmed Langevin's suggestion. Moulin confirmed in particular that an electric field normal to the columns produces a higher current than a field parallel to the track. The recombination in the columnar plasma is so effective that it swamps any initial recombination of freshly separated pairs. Jaffé (1913, 1914) studied the directional effect in greater detail and also investigated the ionization of liquids. For example, in hexane at about 1000 V cm^{-1}, the currents caused by α- and β-particles respectively were found to be $0 \cdot 1\%$ and 10% of the saturation currents produced by the same source in air. For α-particles the ionization current increased in proportion to the component of the field normal to the track. Jaffé also made calculations based on the idea of a critical radius, and obtained theoretical values for the reduction of current due to columnar recombination. Columnar recombination is more effective the higher the

(bimolecular) coefficient of recombination, the greater the density of ions along the track and the smaller their mobility. From this it must be inferred that the efficiency of cathode rays in inducing conductivity increases with their energy and depends critically on the trap-controlled mobility of the carriers.

Jaffé's figures for the ion density in a column in hexane are $4{\cdot}3 \times 10^7$ cm^{-1} for α-particles and $1{\cdot}46 \times 10^5$ cm^{-1} for β-particles. Figures for the energy loss in arsenic trisulphide suggest, with 10 eV per pair created, densities of 8×10^6 cm^{-1} for cathode rays and 8×10^5 cm^{-1} for β-rays—values quite comparable to those found in hexane.

Whilst the mobilities of electrons and holes in many crystals are far greater than those of ions in liquids, the mobility of carriers in amorphous films is trap-controlled or associated with an intermolecular hopping process and probably smaller than that of ions in hexane. The generation of carriers in arsenic trisulphide films by cathode rays and β-rays should therefore have all the features of columnar ionization. For β-rays, as opposed to cathode rays, columnar recombination is reduced owing to the greater separation of the ions and enhanced by the directional effect. The number of carriers released from columnar recombination increases in proportion to the field.

3. *Effect of current density*

Except at very low temperatures, or for very low current density, the gain decreases as the current density increases. The effect is not great. For example, the gain for a specimen of As_2S_3 $4{\cdot}63$ μm thick, at a field of $2{\cdot}2 \times 10^5$ V cm^{-1}, reaches its upper limit of 60 at a current density of 5×10^{-10} A cm^{-2}. At a current density of 5×10^{-7} A cm^{-2} the gain is about 15. Ehrenberg and Ghosh (1969) attribute the reduction of gain to the incidence of Shockley–Read recombination.

4. *High temperature effects*

The EBC gain in a film increases with increasing temperature. Recombination by any one of the three processes referred to is reduced at elevated temperature, and the drift mobility rises, so an increase in gain must be expected. For As_2S_3 a bend occurs in the gain vs. temperature curves above room temperature as shown in Fig. 3.14; a second feature comes into play at about 100°C.

Below 100°C the gain varies reversibly with temperature, i.e. if the temperature returns to a previous value the gain comes back to its original value. Also, on reversal of bias the current changes sign without change in magnitude after a short transition period during which the space charge settles down to a new equilibrium arrangement.

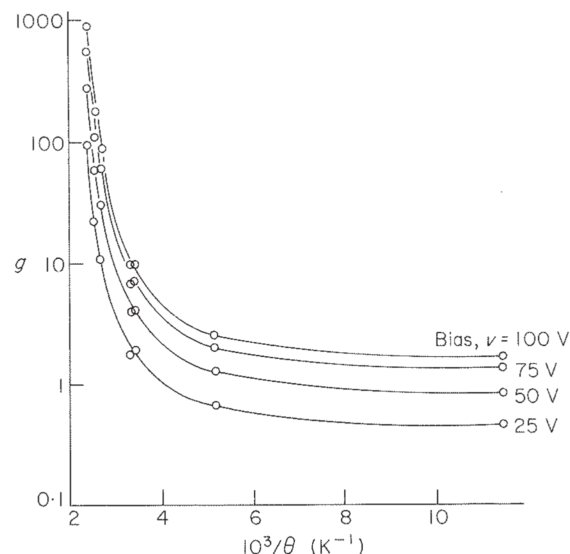

Figure 3.14. The EBC gain g as a function of temperature for an a-As_2S_3 film, with specimen bias v as a parameter. The upturn in this family of curves at about 100°C ($10^3/\theta = 2{\cdot}7$) can be clearly seen; this is accompanied by a rapid increase of g with rising temperature caused by entry of carriers from the electrodes. (Ansbacher and Ehrenberg, 1951)

Above 100°C the gain becomes dependent on the history of the sample. At room temperature, for a field of 9×10^5 V cm^{-1}, the maximum gain measured on a new sample is about 50. After the sample has been heated beyond 100°C and allowed to cool, a gain of several hundred is measured for the same field. Under bombardment this eventually falls by $1{\cdot}3$–$1{\cdot}5$ times, but this is restored to its original value after bombardment at liquid air temperature. Also, above 100°C the increase is accompanied by a kind of switching effect. The current increases initially under bombardment until it stabilizes after seconds or minutes at a "high" value several times its initial value. Once the "high" gain is established for a particular bias and temperature, the EBC current instantaneously follows any variations of the beam. Now, if the polarity of the bias is reversed while the bombardment continues, the gain (in the reverse direction) is initially a small fraction of the previous "high" gain. It then rises slowly to about the magnitude that it had before the reversal of bias. The "high" gain is reached more quickly if the bombarding current is repeatedly interrupted while the bias is kept on. Such "conditioning" of a specimen does not take place without bombardment. Oscilloscope traces showing some of these effects are given in Fig. 3.15.

The difference between low gain and high gain increases with increasing bias and increasing temperature, and it decreases with increasing bombard-

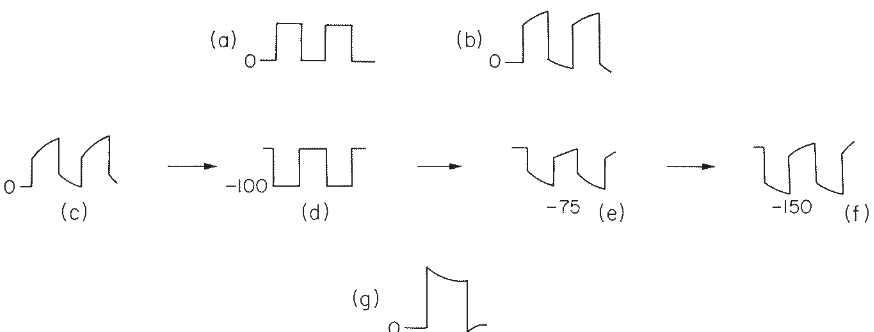

Figure 3.15. Pulsed EBC. (a) represents the bombarding current as a function of time; (b) conduction pulse in a specimen of As_2S_3 at 26°C, with large bias; (c)–(f) conduction pulse in a specimen at 120°C, $I_p = 1{\cdot}4 \times 10^{-7}$ A cm^{-2}. The conduction pulse shape changes on bias reversal: (c) high gain with positive bias; (d) bias merely reversed; (e) negative bias on for 1 s; (f) negative bias on for some time. (g) Al_2O_3 film at 300°C, primary current pulse length 5 ms, $I_p = 2{\cdot}7 \times 10^{-7}$ A cm^{-2}, $V_p = 5$ kV.

ment current and with increasing thickness of the sample. For example, at 0·27 μA cm^{-2} there is no difference between low and high gain below 100°C, but for the very low current density of 1·4 nA cm^{-2} a small effect is already noticeable at 20°C. Also, above 100°C and at low primary energy, the negative high gain can be double the positive gain. This means that the holes travel with less hindrance than the electrons or that the recombination of a mobile electron with an immobile hole is easier than the reverse process. The highest gain on As_2S_3 films is 40 000 at 163°C with $V_p = 24$ kV; this would allow only 0·5 eV for the creation of a pair of carriers.

Appreciable increase of gain with temperature has also been reported for ZnS films. Benoit *et al.* give 25, 60, and 150 as relative values of gains at −100, 50, and 150°C. Ehrenberg and Hidden found that the gain increases 2½-fold between room temperature and 330°C. No secondary effects are mentioned. The threshold, when found, is independent of temperature.

5. *Rise and decay of induced current*

If cathode rays are switched on as a step function, the induced current rises instantly to perhaps half its final value which may be reached after a few milliseconds or hours. It takes longer the lower the bombarding current. For example, with weak β-rays, rise times of up to 4 hours have been observed for As_2S_3 films, and a fraction of an hour for silica. An example is shown in Fig. 3.16. The break between the "prompt" and the "slow" rise is often quite conspicuous. If a build-up of space charge takes place during the slow rise, the increase can turn into a decrease. A reverse process takes place when the bombardment current is switched off.

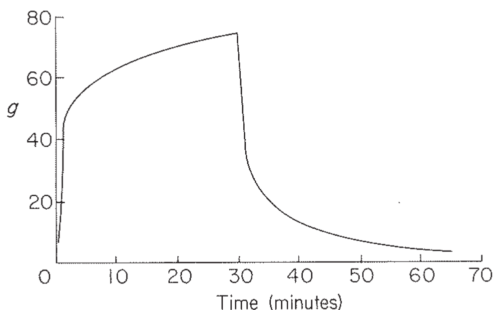

Figure 3.16. Rise and decay of EBC in a thin film of a-As_2S_3 (10·8 μm) when bombarded at a low current density; bias $v = \pm 108$ V, $I_p = 5 \times 10^{-14}$ A cm^{-2}. (Ghosh, 1967)

For the beginning of the slow rise, Alcock (1962) found that the gain for β-rays acting on an As_2S_3 film was proportional to log t for 20 ms $< t <$ 30 s. Hirsch found $g \propto c \tanh(L/t)$ for cathode rays. He suggested (1966) that initially the liberated electrons are trapped by V centres which then become V^- centres capable of neutralizing holes. This process makes up the prompt rise. As the number of V^- centres increases, the density of holes reaches its limiting value during the slow rise. Hirsch carried out his calculation assuming that 10 eV is the average energy required to create a pair, and arrived at the result that the schubweg is small compared with the thickness of the specimen, using likely values for the other parameters—a result that justifies the omission from his calculation of a term denoting the loss of carriers by drift into the electrodes. This omission is no longer justified if, as shown above, the mobilization energy is several hundred volts and the length of the schubweg becomes comparable to the thickness of the specimen. A calculation allowing for this is not at present available.

Figure 3.17(a)–(d) shows how the rise and decay of the EBC under conditions of pulsed beam and steady bias depend on the bias voltage and on the bombarding electron current density in a film of amorphous selenium. Except at low bias and at low current densities, the two-component behaviour is easily seen, and also the change from a rise with time to a fall if the value of V_p is less than the penetration voltage (Spear, 1956). Similar behaviour can be found in thin films of amorphous As_2S_3, and Fig. 3.17(e) is a tracing from a typical oscillograph; in this case the two components cannot be distinguished (Hirsch, 1966). Figure 3.18 shows how the two components can be analysed separately using a log-log plot of the magnitude of the prompt components of gain (g_0) and the slow component (g_s) as a function of bombarding current density (I_p) when the beam is totally penetrating. The slopes of the two double-logarithmic plots are ½ and 1, so indicating that a bimolecular recombination process is responsible for the kinetic behaviour

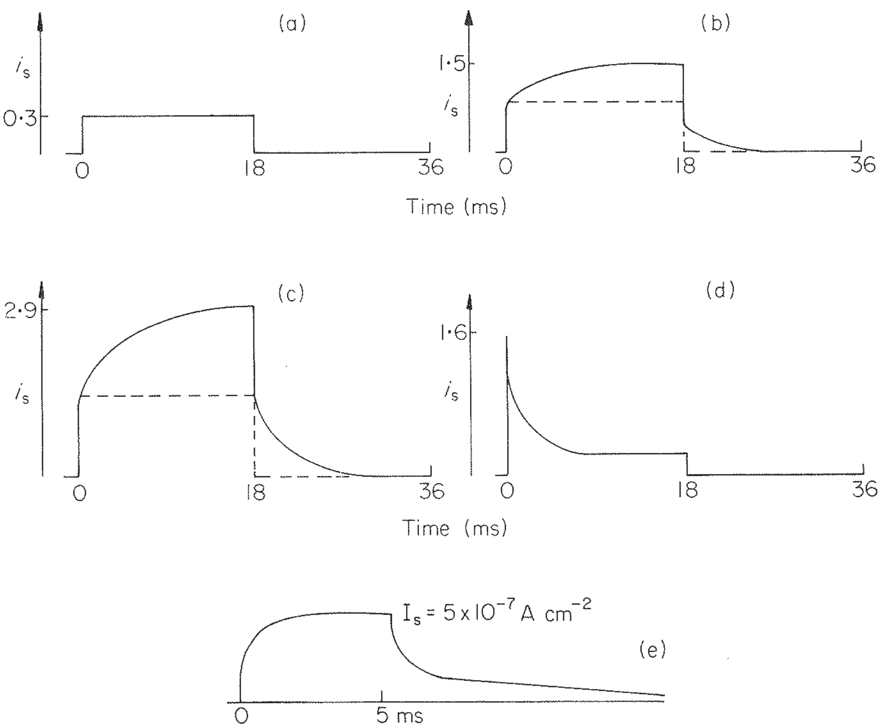

Figure 3.17. Growth and decay of induced current in a-Se [(d) $V_p = 10$ kV, $i_p = 4 \times 10^{-9}$ A; (a)–(c) $V_p = 45$ kV, $i_p = 8 \times 10^{-10}$ A]: (a) bias $v = 30$ V, (b) $v = 70$ V, (c) $v = 100$ V, (d) $v = 45$ V. (Spear, 1956) (e) Trace of typical oscillogram for a 4·3 μm film of a-As_2S_3 at room temperature when $V_p = 50$ kV, $I_p = 10^{-8}$ A cm^{-2}, and the bias field was $2{\cdot}5 \times 10^5$ V cm^{-1}. (Hirsch, 1966)

of the slow component, whereas a monomolecular process is applicable to the prompt component (Hirsch, 1966). These two can therefore be attributed to the primary and secondary EBC processes respectively.

6. The nature of EBC materials

There is no doubt that the conductivity induced by electron bombardment varies from material to material. Mica shows no induced conductivity whereas some plastics films retain the bombarding charge of electrons almost indefinitely at the location where they originally came to rest. Normally, materials that do not show induced conductivity are not very sensitive to impurities; this is in conformity with the often quoted statement that amorphous semiconductors cannot be doped (Mott and Davis, 1971). However, Spear and Le Comber (1975) have shown that, in one amorphous solid

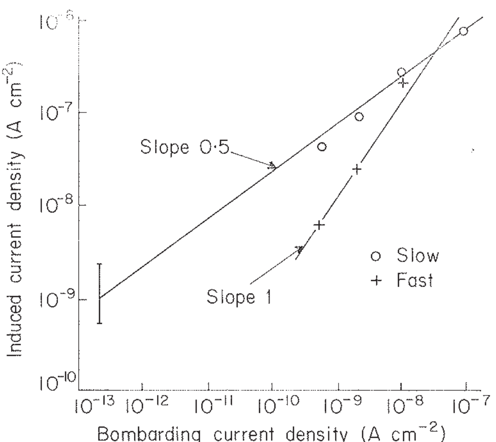

Figure 3.18. Separation of fast and slow components of rise and decay of EBC. Double-logarithmic plot of induced current density as a function of bombarding current density in As_2S_3 evaporated film 4·3 μm thick bombarded by 50 keV electrons, except for the lowest value where β-particles were used. Notice the bimolecular nature of the slow component compared with the monomolecular nature of the fast component. (Hirsch, 1966)

at least, it is possible to add impurities substitutionally to form either n-type or p-type amorphous silicon. It should be mentioned that this does not make it less necessary to use pure and well defined materials, since certain impurities may make films leaky and liable to breakdown. Normally the experimentalist will use the purest material commercially available, or try to improve on it; for example, As_2S_3 is easily purified by molecular sublimation (Bowlt, 1967), and ZnS can be purchased as "phosphor quality".

A notable dependence of EBC gain on impurities was observed for fused silica by Ehrenberg *et al.* (1966); the specimens had the shape of microscope cover slips and were exposed to β-rays from a Sr-90 radioactive source. The electrons lost only a fraction of their initial energy in the specimens and thus caused uniform ionization; no induced conduction was observed in silica-rich glass, but this may have been masked by its very high leakage. Natural fused silica gave a gain of unity at 500 V bias, Vitreosil (natural silica purified by electrolysis but retaining 50 parts per million Al) gave a gain of about 5, and Spectrosil WF (produced by vapour phase hydrolysis of silicon tetrachloride, with 500 parts per million Cl as main impurity) gave a gain of about 15; an alternative process gave Spectrosil with 4000 parts per million OH, but much less Cl, which showed a gain in the neighbourhood of 100. It should be remembered that Pensak previously had observed gain of the same order on thin silica films produced by decomposition of ethyl silicate vapour.

Films of amorphous selenium behave in many respects differently from "normal" films but share with them the property of giving two rates of rise. At low bias the "slow" rise is absent, as shown in Fig. 3.17(a). As the bias is increased, the "prompt" rise grows to a limiting value whilst the "slow" rise develops and grows. Spear suggested that the prompt rise represents the current due to pairs created by the primary electrons, and that the slow rise is due to injected carriers. He reports that the limiting value of the fast rise leads to the same value of E^* (energy of pair creation) as the saturation value of the positive gains at low electron energy, a coincidence confirming this value for E^* and the interpretation of the fast rise. If we accept this interpretation we are tempted to ask if the same idea could apply to materials like As_2S_3. Figure 3.17(e) shows that in As_2S_3 the fast rise is also absent at high bias.

The general equations for the rise and decay of induced conductance in the case of a bimolecular recombination process can be derived from the general kinetic equations. If the generation rate is β pairs $cm^{-3}\,s^{-1}$, and the recombination law is of the form αnp, we can put the recombination rate as αn^2 if one sign of carrier is not immediately trapped. Thus, during generation,

$$dn/dt = \beta - \alpha n^2 \tag{3.1}$$

This has the solution, given the boundary conditions $n = 0$ when $t = 0$,

$$n = (\beta/\alpha)^{1/2} \tanh\, (\alpha\beta)^{1/2} t \tag{3.2}$$

In the steady state (i.e. $t \to \infty$), $n = (\beta/\alpha)^{1/2}$. The decay law and its solution are given by the equations

$$dn/dt = -\alpha n^2 \tag{3.3}$$

$$n = 1/(1/n_0 + \alpha t) \tag{3.4}$$

where n_o is the initial concentration of carriers. This relationship approximates to $n \approx 1/\alpha t$ as $t \to \infty$.

Thus it is seen that, where the conduction mechanism is dominated by bimolecular recombination, the rise and decay process is approximately hyperbolic. The tangent to the current rise curve at $t = 0$ meets the tangent for $t = \infty$ at $t_r = (\beta\alpha)^{1/2}$. Similarly, the tangent to the current decay curve meets the line $n = 0$ at a time t_r after the excitation has been turned off.

Variations in equations (3.2) and (3.4) occur if trapping, trap distributions, and detrapping are taken into account.

C. Lateral induced conductivity

If the direction of incidence of the bombarding electrons is perpendicular to the direction of induced currents, we can describe this EBC effect as lateral

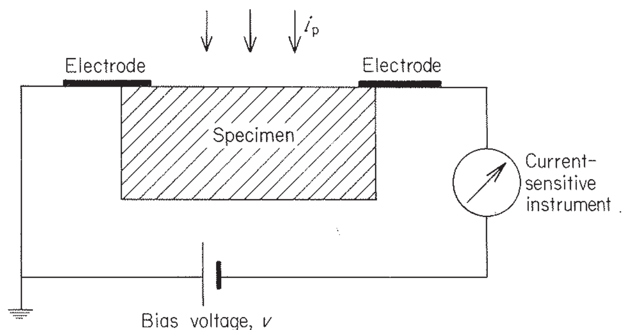

Figure 3.19. Disposition of electron beam, surface of specimen, and electrodes in the case of lateral EBC.

induced conductivity; the arrangement of the beam and the specimen is shown in Fig. 3.19.

Selenium, and the photoconductivity of its grey (metallic) modification, were discovered in the 19th century. Simple cells are made by painting or pressing molten selenium just above its melting point on to a glass plate provided with electrodes; such cells remained more or less a curiosity because their response to light is sluggish and unreliable. It occurred to Ralph de Laer Krönig (1924) that electron bombardment should have the same effect as illumination. He placed a cell of 3500 ohm dark resistance, forming an arm of a Wheatstone bridge, in the position of the anode of a thermionic triode and examined the change in resistance as a function of anode voltage and current; the resistance was reduced to half the dark value at 90 V anode potential and 400 μA anode current.

Although the grey metallic form had been known for a long time to be photoconductive, it was Weimer (1950) and Bixby and Ullrich (1951) independently who discovered that amorphous selenium also possesses this property. The amorphous form is produced by vacuum evaporation on to a cold substrate, or a substrate certainly no warmer than 50°C. The EBC of this form was described by Pensak simultaneously with Weimer's description of the photoconductivity.

1. Surface layers

Unless the bombarding electrons are very energetic, the excitation of a thick specimen is limited to a shallow region near the surface. The path of the electrons and holes liberated internally by the primary beam is limited to a region determined by their free lifetime.

Lateral EBC in crystals of CdS, CdSe, CdTe, and ZnSe, and in thin layers of CdSe and CdTe, was studied by Kot and Simashkevich (1962). The thin layers of CdSe and CdTe were "sensitized" by heating the layers in an

oxygen atmosphere; this reduced the dark current and increased the EBC gain by forming "traps" (activation centres). The entire gap between the electrodes was bombarded with electrons. It was found that the most responsive crystals were those with smooth surfaces, and the least sensitive those with transverse grooves. Typical values for the EBC gain are given in Table 3.1, from which it is seen that the sensitizing procedure on the last

Table 3.1. Lateral EBC gain for a variety of specimens when the entire gap between the electrodes is bombarded; $V_p = 3$ kV, $i_p = 5 \times 10^{-8}$ A.

Specimen	Form	Gain
CdS	crystal	10
CdSe	crystal	10
CdTe	crystal	0·5
ZnSe	crystal	0·04
CdTe	layer	0·5
CdSe	layer	2×10^3

specimen mentioned clearly had a pronounced effect. A similar effect in thin evaporated films of CdS was reported by Gibbons (1974b); a (secondary) EBC gain of several thousand could be obtained by doping with Cu followed by an air-bake. Kot and Simashkevich found that the induced conductance varied linearly with i_p at low values of current, and that with increasing V_p the gain rose approximately hyperbolically. This was interpreted as due to an increase in the carrier lifetime as the generated carriers were then further away from the surface.

Soon after the discovery by McKay (1949) that the region near the contact of a germanium point-contact diode was sensitive to bombardment by α-particles, similar effects were found when the experiment was repeated but instead using electron bombardment (Moore and Hermann, 1951). This is a very important forerunner of a valuable number of effects associated with electron bombardment of semiconductor p–n junctions which will be described in detail under the heading "electron voltaic effect" in Chapter 4, and it provides the basis for obtaining images from a scanning electron microscope when used in the EBIC mode (Holt *et al.*, 1974).

It is interesting that Ansbacher (1950) was unable to detect lateral induced conductivity in electron bombarded layers of ZnS, glass, mica, natural ruby, electrolytic Al_2O_3, and coloured or uncoloured alkali halide crystals.

Further measurements of the lateral EBC of single crystals of CdS with Aquadag contacts were made by Archangelskaya and Bonch-Bruevich (1951). The entire gap between the electrodes was bombarded, and the induced currents were measured with a steady dc bias. The dark conductance of the CdS was 5×10^{11} ohm-cm and $V_p = 2$ kV for all the experiments; the bombarding current density was between 1 and 15 μA cm^{-2}. All measurements were made after an initial conditioning period of electron bombardment lasting 15 minutes; after this process there was no hysteresis in the conductivity decay rates when the beam was interrupted, and reproducible results could thereafter be obtained for periods of several days provided that i_p was not increased beyond that needed for conditioning.

It was found that approximately $\Delta\sigma_0 \propto i_p^{1/2}$ where $\Delta\sigma_0$ is the steady value of increased specimen conductance in the presence of bombardment. Also, when the beam was interrupted, the induced conductance decayed with a time constant $\tau_m \propto i_p^{1/2}$. It did not decay according to a bimolecular model, but an accurate expression

$$\Delta\sigma = \Delta\sigma_0/(1 + at)^{\alpha} \tag{3.5}$$

was found to apply, where $a = 500$ s^{-1} and $\alpha = 0{\cdot}65$. The increase in decay time constant with time, as shown by equation (3.5), is often found in a large number of photoconductors and of phosphors.

The presence of an insensitive surface layer on single crystals of CdS when subjected to electron bombardment was demonstrated by Ryvkin *et al.* (1954). It was found that in single crystals from different sources, and in thick polycrystalline layers, the beam had to penetrate a thickness of between 100 and 1000 Å before the induced conductance rose rapidly with increasing V_p (see Fig. 3.20). The authors suggested that the fall in sensitivity near the surface was connected with an increase in recombination rate due to defects associated with an adsorbed surface layer.

Experiments on thin layers of ZnO, produced by oxidizing evaporated zinc, have provided valuable evidence for the kinetics of the process by which this compound loses oxygen under the influence of exciting radiation, as well as incidental data on the EBC; Heiland (1952) distinguished them as the "slow" process and the "fast" process respectively. Figure 3.21 shows how the induced current ("fast" process) responds to a step-function of bombardment. The thickness of the layer before baking in air at 400°C for 5 min to form the oxide was between 0·06 and 0·25 μm for different specimens, and the bombarding electrons had a set energy in the range of 1–6 keV. The results show EBC gain of about 100 at i_p about 6×10^{-7} A; it rose to a steady value within about 0·5 ms. The primary beam irradiated the entire space between the contacts as well as a large proportion of the contacts themselves (zinc contacts). As mentioned, the "slow" process

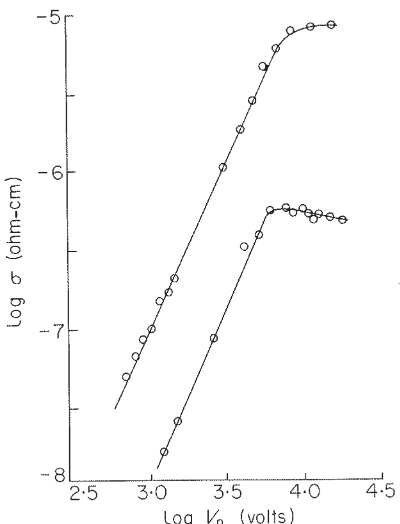

Figure 3.20. Induced lateral conductance as a function of bombarding voltage for two different single crystals of CdS. (Ryvkin *et al.*, 1954)

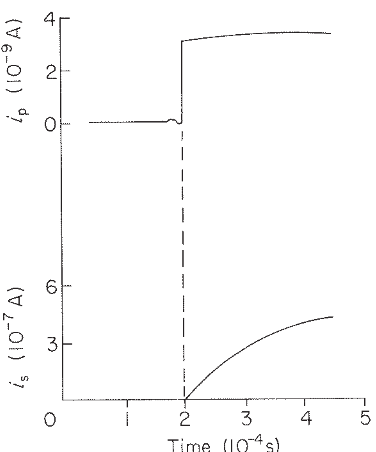

Figure 3.21. The lateral EBC for the fast process in a zinc oxide layer, showing (above) the exciting electron beam current waveform and (below) the corresponding rise in induced current with time. (Heiland, 1952)

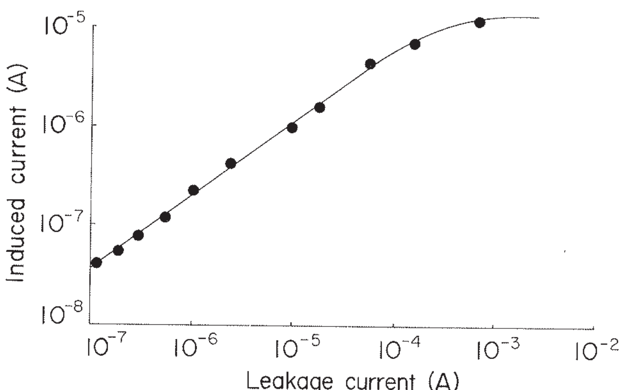

Figure 3.22. Dependence of the lateral induced current on the leakage current in a thin film of ZnO when the increased leakage arises through loss of oxygen; bias 10 V, $I_p = 3{\cdot}2 \times 10^{-7}$ A cm^{-2}, layer thickness 0·06–0·25 μm, $V_p = 5$ kV. (Heiland, 1952)

represents a loss of oxygen from the lattice under the influence of excitation; the resulting oxygen vacancies act as donors and the leakage current then rises. Figure 3.22 shows how the induced current depends on the leakage for a constant electron excitation intensity of $1{\cdot}6 \times 10^{-3}$ W cm^{-2}; it was found that the gain depends on the leakage current as $g \propto i_l^{0{\cdot}77}$ and on the bombarding current as $g \propto i_p^{-0{\cdot}60}$ approximately. These results agree substantially with the photoconductivity results by Mollwo (1948).

Sverdlova and Rokakh (1964) also exposed films of ZnO (0·4–0·8 μm thick) and of CdS (0·4–4 μm thick) to electron bombardment currents of 10^{-5}–10^{-8} A, at energies up to 5 keV. The ZnO films again were prepared by evaporation of Zn and subsequent oxidation; the gap between the electrodes was about 7 mm. Changes of resistance by factors of 10^4–10^5 were observed, some of which were due to chemical changes such as loss of oxygen.

Only one measurement of the lateral EBC of a thin-layer photoemissive cathode has been published. An antimony–caesium photocathode was studied under electron excitation with $V_p = 600$ V (Safratova-Eskertova, 1955); it was found that $i_s \propto i_p^{1/2}$, and in the range 10^{-10}–10^{-11} A gains of several thousand were obtained.

The earlier experiments by de Laer Krönig on the EBC of a selenium photocell were repeated by Rittner (1948) using electrodes made of tungsten wire spaced by 5 mm. Under a dc bias of 225 V he measured steady values of g equal to 63 and 123 respectively when the bombarding voltage was 1·0 and 2·0 kV; the bombarded area was only 1 mm in diameter but the published data make no reference to the influence of the position of the beam.

2. Position of the beam and the influence of contacts

A very important feature of the lateral EBC effect in insulators is the way in which the gain varies with the position of the beam between the electrodes. Experiments have provided valuable evidence for the existence of space charges due to trapped carriers or ionized impurities in the immediate vicinity of the contacts. The lateral induced conductivity of single crystals of CdS between 20 and 30 μm thick was measured by Benda (1951) using gold or silver electrodes between 1 and 3 mm apart for the various specimens, with bombarding voltages in the range of 800 V to 3 kV. The induced conduction current i_s varied with the position of the beam on the specimen; it increased markedly when the beam moved from the centre to the edge of the gap between the electrodes, and maxima were observed when the beam actually touched them. The maximum was higher when the electron beam hit the positive side, and this indicates that diffusion of excitons and production of light or X-rays is not a likely explanation for the higher gain near the contacts. Additional measurements in this series showed that $i_s = k i_p{}^a V_p{}^b$ where the constants a and b have values of 0·61–0·88 and 1·1–3·7 respectively and k is an arbitrary constant.

The experimental results of Kot and Simashkevich are summarized in Fig. 3.23 in the case where the contacts of gold or silver to CdS are rectifying. If ohmic (injecting) contacts are used the influence of the position of the beam is the opposite of that just described; for example, if indium or gallium

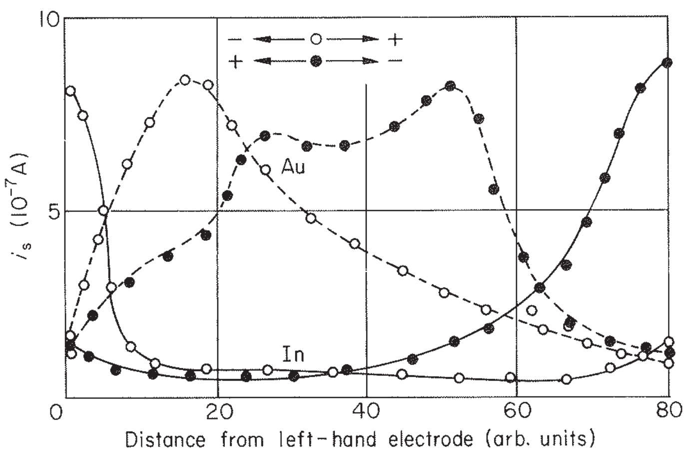

Figure 3.23. The influence of contacts and the position of the beam in the case of lateral EBC, for specimens of CdS or CdSe with In or Au electrodes; note the enhanced EBC when the beam strikes the In contact when it is biased negatively whereas there is a marked drop in the EBC if the beam approaches a negative Au contact. (Kot and Simashkevich, 1962)

contacts are used, i_s rises to a maximum when the beam strikes the negative side. If mixed contacts are employed, such as gold or silver with indium or gallium, the dark current is unsymmetrical and it is found that the highest value of i_s occurs when the region in the vicinity of the negative contact is excited, although when the "diode" is reverse biased the maximum value of i_s occurs when the position of the beam is slightly nearer the centre of the gap than in the case when it is forward biased. The latter experimental results are shown on the same figure for comparison.

Ehrenberg and Shrivastava (1973) showed that surface and volume induced currents could be detected simultaneously in 0·5 mm thick single crystals of ZnS. The surface currents were carried by "channels", and the volume currents were due to carriers with a bulk drift length of about 200 μm. The surface currents arose mainly as a result of built-in fields, and their influence could be suppressed by using a guard ring electrode.

D. The influence of contacts in normal EBC

As might have been expected, the influence of the contacts (and the relative position of the beam) is more important in lateral EBC than in the case where the exciting electrons penetrate the sample completely and we are interested only in the conductivity through its thickness. Obviously, if the electrode metal is thick (in units of mass/area) it will absorb more energy from the beam, and in this way the variation of g with V_p as a function of electrode thickness can be easily understood. This will be discussed in Chapter 7 where the influence of the thickness of a gold top (bombarded) electrode will be shown (Fig. 7.15).

If the specimen is capable of exhibiting significant EBC without the need for complete beam penetration, the contacts can have an important effect. An example showing this is single-crystal CdS; aluminium or indium form injecting contacts whereas graphite or gold form rectifying contacts because current transport is mainly by electrons. If crystals about 30 μm thick are fitted with two aluminium, gold, or indium contacts, on opposite faces, the gain at bombarding voltages of about 30 kV is about the same for any contact metal. However, if the specimen is not symmetrical, such as may be the case when one contact is of indium and the other of gold or graphite, the "dark" current characteristic is asymmetric and the EBC gain is higher if the bombarded contact is negative with respect to the other (Gibbons, 1974b). Trodden and Jenkins (1965) also found that symmetrical specimens of CdS with Au–Au or In–In contacts yield higher g values if the bombarded contact is negative with respect to the unbombarded one; this result is the opposite of that found by Benda for lateral EBC.

These results confirm that, even in the dark, conduction currents in single

crystals of CdS are determined by the electron injecting properties of the metallic contact. The ability of the negative contact to supply electrons is promoted by electron excitation, and this explains why a normally non-injecting gold electrode can be rendered effective as an injector of electrons when it is bombarded. A similar promotion occurs if the bombarded contact is made from graphite (Aquadag). Electron bombardment of a negatively biased graphite contact can make it so effective that the EBC gain is then higher than when the specimen is turned so that the indium contact faces the beam; this is probably because near the negative contact the space charge barrier (which also limits the dark current) is nearer the contact when the graphite is biased negatively.

From these experiments it is clear that contacts (if they are thin) affect normal EBC only in the case of materials like CdS where appreciable EBC in the steady state can occur with a non-penetrating beam. In these circumstances a higher EBC is obtained when the bombarded contact is biased in such a direction that this contact injects the more mobile carrier. A higher ratio of induced current to dark current is obtained if the electrodes are different, the specimen is back-biased, and the non-injecting contact is bombarded. This seems also to apply to evaporated thin films of CdS, because in this material intercrystalline barriers are not a serious impediment to steady current flow beyond the penetrated region.

4

The electron voltaic effect (EVE)

I. Semiconductor junctions

In a semiconductor, near a metal electrode, or where differently dope regions come together, i.e. at a junction, the potential energy of carrier changes; this difference in potential prevents holes from crossing into th n-region and electrons into the p-region. The potential necessary to establ ish thermodynamic equilibrium is increased if the junction is back-biased The potential energy diagrams for biased Schottky-barrier and p–n junc tions are shown in Figs. 4.1 and 4.2 respectively. A depletion region is result of all the donors or acceptors being fully ionized, and the free carrier liberated from them being drawn out of the region near the junction. A accumulation region represents the opposite situation—carriers are attrac ted to the junction and the donors or acceptors revert to their unionize state. Such junctions are rectifying, and are sources of an emf whe irradiated by light which produces a photoelectric effect in the material Units designed for this purpose (Fig. 4.3) are called photoelements o photovoltaic cells, but all p–n junctions respond to ionizing radiation.

The behaviour of photovoltaic cells under light excitation has been briefl mentioned in Chapter 3. The equivalent phenomenon when electron excita tion is used (known as the electron voltaic effect or EVE) differs from th photovoltaic effect mainly owing to the non-exponential absorption o energy from the beam and complete freedom of choice of the energy of th ionizing particle (photon or electron energy). For reasons such as these, th beam energy can often be chosen to be a high multiple of the mobilizatio energy. Selenium photoelements were shown by Becker and Kruppk (1937) to be sensitive to bombardment by fast electrons. McKay (1951 reported the decrease in resistance of the barrier associated with a poin contact to germanium when bombarded by α-particles. In such devices th values of g can be very high. The EVE is of importance in devic applications, especially when the junction is back-biased to reduce it capacitance and to increase the width of the most sensitive region. Suc applications will be discussed in Chapter 7.